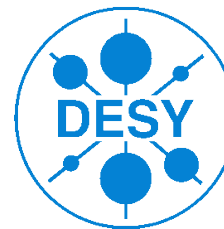
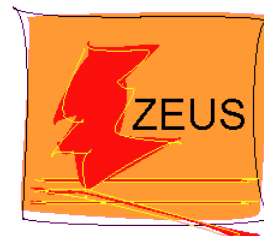


Precision QCD measurements at HERA

Daniel Britzger
for the H1 and ZEUS collaborations

Determination of the Fundamental Parameters in QCD Workshop
Mainz, Germany
08.03.2016



Deep-inelastic scattering

Kinematic variables

- virtuality of exchanged boson

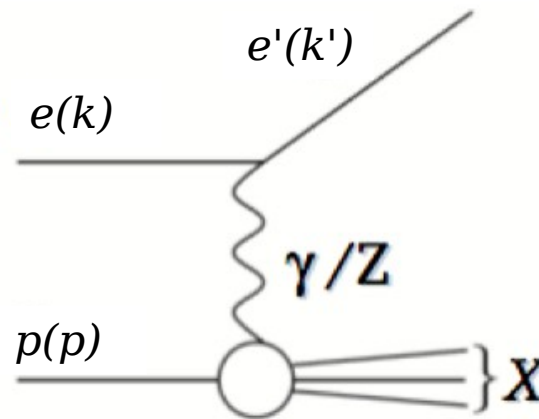
$$Q^2 = -q^2 = -(k - k')^2$$

- Bjorken scaling variable

$$x = \frac{Q^2}{2 p \cdot q}$$

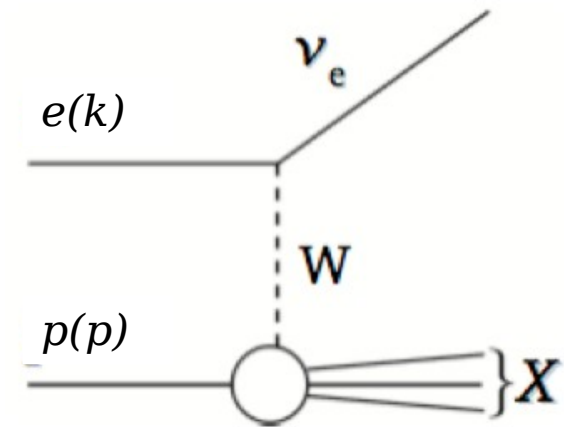
Neutral current scattering

$$ep \rightarrow e'X$$



Charged current scattering

$$ep \rightarrow \nu_e X$$



Factorization in ep collisions

$$\sigma_{ep \rightarrow eX} = \int f_{p \rightarrow i} \otimes \hat{\sigma}_{ei \rightarrow eX}$$

$x f_{p \rightarrow i}$ = quark/gluon momentum density in proton:
Parton density functions (PDFs)

PDFs are not observables – only structure functions are

Measuring these cross sections allows indirect access to the universal PDFs, which are also valid for pp collisions

Structure functions

$$\frac{d\sigma_{NC}^{\pm}}{dx dQ^2} = \frac{2\pi\alpha^2}{x} \left[\frac{1}{Q^2} \right]^2 \left[Y_+ \tilde{F}_2 \mp Y_- x \tilde{F}_3 - y^2 \tilde{F}_L \right]$$

$$Y_{\pm} = 1 \pm (1-y)^2$$

$$\frac{d\sigma_{CC}^{\pm}}{dx dQ^2} = \frac{G_F^2}{4\pi x} \left[\frac{M_W^2}{M_W^2 + Q^2} \right]^2 \left[Y_+ \tilde{W}_2^{\pm} \mp Y_- x \tilde{W}_3^{\pm} - y^2 \tilde{W}_L^{\pm} \right]$$

DIS cross sections are expressed in terms of structure functions

Dominant contribution from F_2 structure function

$$\tilde{F}_2 \propto \sum (xq_i + x\bar{q}_i)$$

Relevant at high $Q^2 \sim M_Z^2$

$$x\tilde{F}_3 \propto \sum (xq_i - x\bar{q}_i)$$

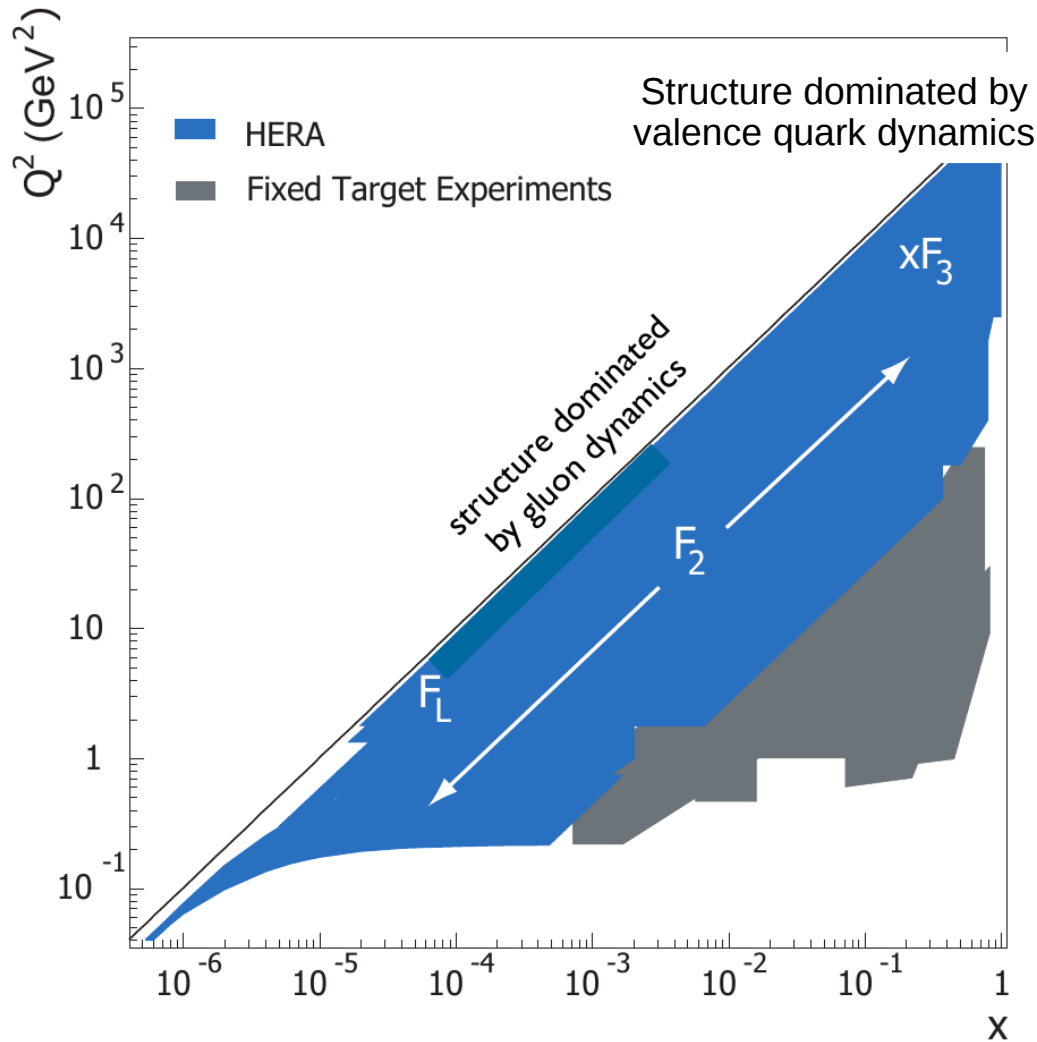
Sensitive at low Q^2 and high y

$$\tilde{F}_L \propto \alpha_s \cdot xg(x, Q^2)$$

Measured cross sections are reduced cross sections

Measurement is a direct determination of the structure functions

HERA kinematic plane



HERA data cover a wide kinematic region of x, Q^2

NC measurements

- F_2 dominates most of Q^2 reach
- xF_3 contributes to EW regime
- F_L contributes only at highest y

CC measurements

- W_2 and xW_3 contribute equally
- W_L only at high y

LHC: largest mass states at large x

For central production $x_1=x_2$

$$M = x\sqrt{s}$$

i.e. $M > 1\text{TeV}$ probes $x > 0.1$

High- x predictions rely on

- data (DIS / fixed target)
- sum rules
- behaviour of PDFs as $x \rightarrow 1$

HERA operation

HERA-I operation 1993-2000

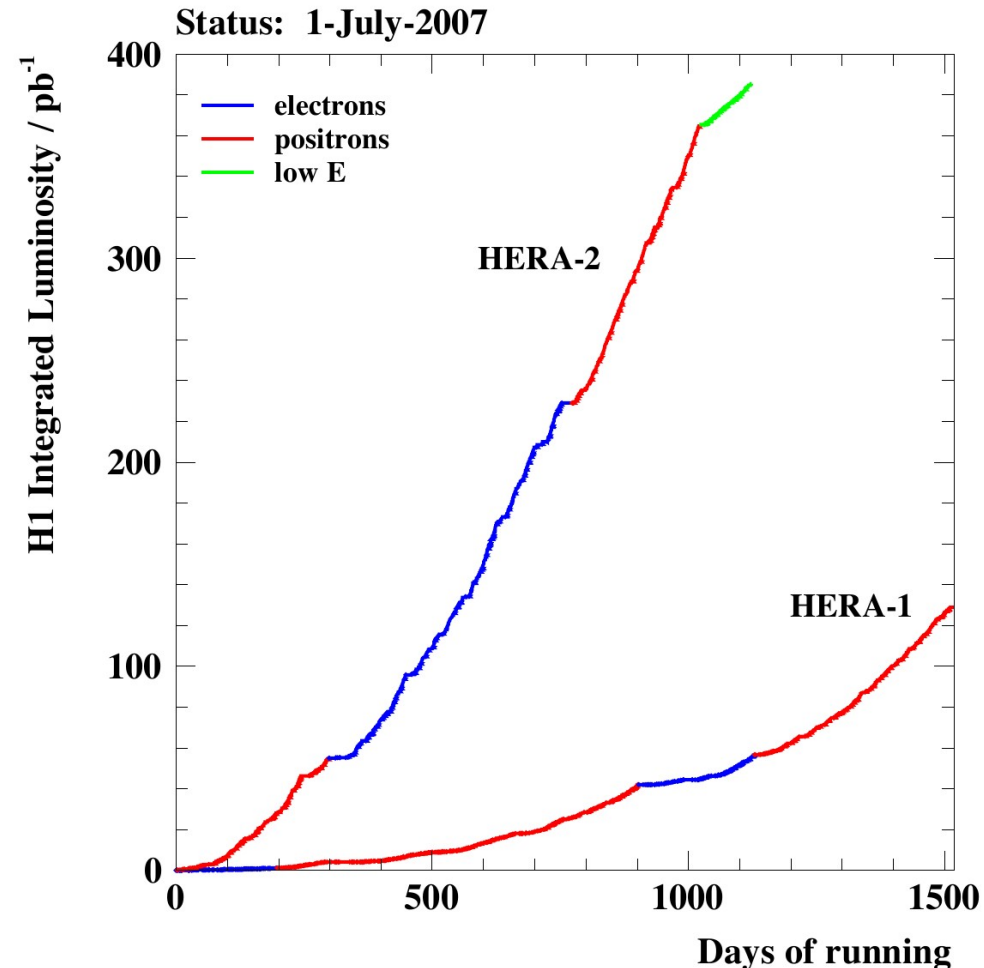
- $E_e = 27.6$ GeV
- $E_p = 820 / 920$ GeV
- $\sqrt{s} = 301$ & 318 GeV
- int. Lumi. ~ 110 pb⁻¹ per experiment

HERA-II operation 2003-2007

- $E_e = 27.6$ GeV
- $E_p = 920$ GeV
- $\sqrt{s} = 318$ GeV
- int. Lumi. ~ 330 pb⁻¹ per experiment
- Longitudinally polarised leptons

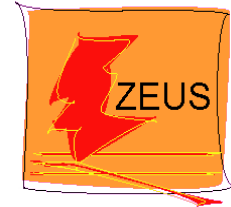
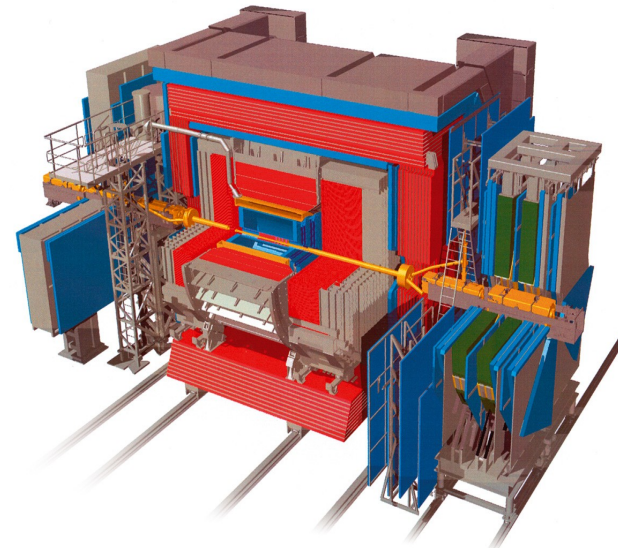
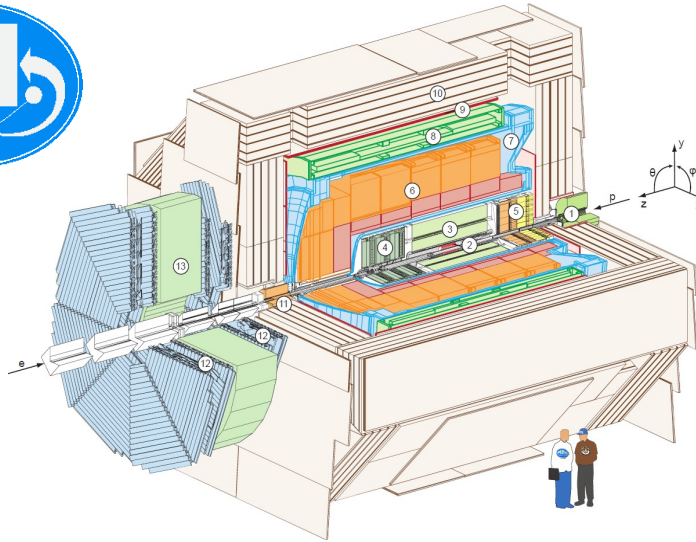
Low-Energy Run 2007

- $E_e = 27.6$ GeV
- $E_p = 575$ & 460 GeV
- $\sqrt{s} = 225$ & 251 GeV
- Dedicated F_L measurement



H1 and ZEUS

Two multi-purpose collider experiments: H1 and ZEUS



High statistics

- Luminosity: approx. 0.5 fb^{-1} per experiment

Excellent control over experimental uncertainties

- Overconstrained system in DIS
- Electron measurement: 0.5 – 1% scale uncertainty
- Jet energy scale: 1%
- Trigger and normalization uncertainties: 1-2 %
- Luminosity: 1.8 – 2.5%

HERA structure function data

Data Set	x_{Bj} Grid		Q^2 [GeV ²] Grid		\mathcal{L} pb ⁻¹	e^+/e^-	\sqrt{s} GeV	x_{Bj}, Q^2 from equations	Ref.	
	from	to	from	to						
HERA I $E_p = 820$ GeV and $E_p = 920$ GeV data sets										
H1 svx-mb [2]	95-00	0.000005	0.02	0.2	12	2.1	e^+p	301, 319	13,17,18	[3]
H1 low Q^2 [2]	96-00	0.0002	0.1	12	150	22	e^+p	301, 319	13,17,18	[4]
H1 NC	94-97	0.0032	0.65	150	30000	35.6	e^+p	301	19	[5]
H1 CC	94-97	0.013	0.40	300	15000	35.6	e^+p	301	14	[5]
H1 NC	98-99	0.0032	0.65	150	30000	16.4	e^-p	319	19	[6]
H1 CC	98-99	0.013	0.40	300	15000	16.4	e^-p	319	14	[6]
H1 NC HY	98-99	0.0013	0.01	100	800	16.4	e^-p	319	13	[7]
H1 NC	99-00	0.0013	0.65	100	30000	65.2	e^+p	319	19	[7]
H1 CC	99-00	0.013	0.40	300	15000	65.2	e^+p	319	14	[7]
ZEUS BPC	95	0.000002	0.00006	0.11	0.65	1.65	e^+p	300	13	[11]
ZEUS BPT	97	0.0000006	0.001	0.045	0.65	3.9	e^+p	300	13, 19	[12]
ZEUS SVX	95	0.000012	0.0019	0.6	17	0.2	e^+p	300	13	[13]
ZEUS NC [2] high/low Q^2	96-97	0.00006	0.65	2.7	30000	30.0	e^+p	300	21	[14]
ZEUS CC	94-97	0.015	0.42	280	17000	47.7	e^+p	300	14	[15]
ZEUS NC	98-99	0.005	0.65	200	30000	15.9	e^-p	318	20	[16]
ZEUS CC	98-99	0.015	0.42	280	30000	16.4	e^-p	318	14	[17]
ZEUS NC	99-00	0.005	0.65	200	30000	63.2	e^+p	318	20	[18]
ZEUS CC	99-00	0.008	0.42	280	17000	60.9	e^+p	318	14	[19]
HERA II $E_p = 920$ GeV data sets										
H1 NC ^{1.5p}	03-07	0.0008	0.65	60	30000	182	e^+p	319	13, 19	[8] ¹
H1 CC ^{1.5p}	03-07	0.008	0.40	300	15000	182	e^+p	319	14	[8] ¹
H1 NC ^{1.5p}	03-07	0.0008	0.65	60	50000	151.7	e^-p	319	13, 19	[8] ¹
H1 CC ^{1.5p}	03-07	0.008	0.40	300	30000	151.7	e^-p	319	14	[8] ¹
H1 NC med Q^2 ^{*y,5}	03-07	0.0000986	0.005	8.5	90	97.6	e^+p	319	13	[10]
H1 NC low Q^2 ^{*y,5}	03-07	0.000029	0.00032	2.5	12	5.9	e^+p	319	13	[10]
ZEUS NC	06-07	0.005	0.65	200	30000	135.5	e^+p	318	13,14,20	[22]
ZEUS CC ^{1.5p}	06-07	0.0078	0.42	280	30000	132	e^+p	318	14	[23]
ZEUS NC ^{1.5}	05-06	0.005	0.65	200	30000	169.9	e^-p	318	20	[20]
ZEUS CC ^{1.5}	04-06	0.015	0.65	280	30000	175	e^-p	318	14	[21]
ZEUS NC nominal ^{*y}	06-07	0.000092	0.008343	7	110	44.5	e^+p	318	13	[24]
ZEUS NC satellite ^{*y}	06-07	0.000071	0.008343	5	110	44.5	e^+p	318	13	[24]
HERA II $E_p = 575$ GeV data sets										
H1 NC high Q^2	07	0.00065	0.65	35	800	5.4	e^+p	252	13, 19	[9]
H1 NC low Q^2	07	0.0000279	0.0148	1.5	90	5.9	e^+p	252	13	[10]
ZEUS NC nominal	07	0.000147	0.013349	7	110	7.1	e^+p	251	13	[24]
ZEUS NC satellite	07	0.000125	0.013349	5	110	7.1	e^+p	251	13	[24]
HERA II $E_p = 460$ GeV data sets										
H1 NC high Q^2	07	0.00081	0.65	35	800	11.8	e^+p	225	13, 19	[9]
H1 NC low Q^2	07	0.0000348	0.0148	1.5	90	12.2	e^+p	225	13	[10]
ZEUS NC nominal	07	0.000184	0.016686	7	110	13.9	e^+p	225	13	[24]
ZEUS NC satellite	07	0.000143	0.016686	5	110	13.9	e^+p	225	13	[24]

H1 & ZEUS have published all datasets

- HERA-I
- HERA-II at high Q^2
- HERA-II at reduced centre-of-mass energies

Data combination

- 41 datasets are combined
 - NC & CC cross sections
 - e+p & e-p scattering
 - 4 values of \sqrt{s}
- 2927 input data points
- 1307 combined points
- data points are swum to common (x, Q^2) -grid points:

$$\sigma(x_{grid}, Q_{grid}^2) = \frac{\sigma_{model}(x_{grid}, Q_{grid}^2)}{\sigma_{model}(x_{meas}, Q_{meas}^2)} \cdot \sigma_{meas}(x_{meas}, Q_{meas}^2)$$

The usage of different reconstruction techniques and the differences in the strengths of the detector components of the two experiments lead to a substantial reduction of the systematic uncertainties of the combined cross sections.

H1 & ZEUS data combination

Combination of all H1 and ZEUS datasets

- 2927 data points → 1307 combined points
- *HERAAverager* package used
- Correlations of systematic uncertainties fully considered
- Minimisation procedure based on χ^2 definition

$$\chi_{\text{exp},ds}^2(\mathbf{m}, \mathbf{b}) = \sum_i \frac{[m^i - \sum_j \gamma_j^i m^i b_j - \mu^i]^2}{\delta_{i,\text{stat}}^2 \mu^i (m^i - \sum_j \gamma_j^i m^i b_j) + (\delta_{i,\text{uncor}} m^i)^2} + \sum_j b_j^2$$

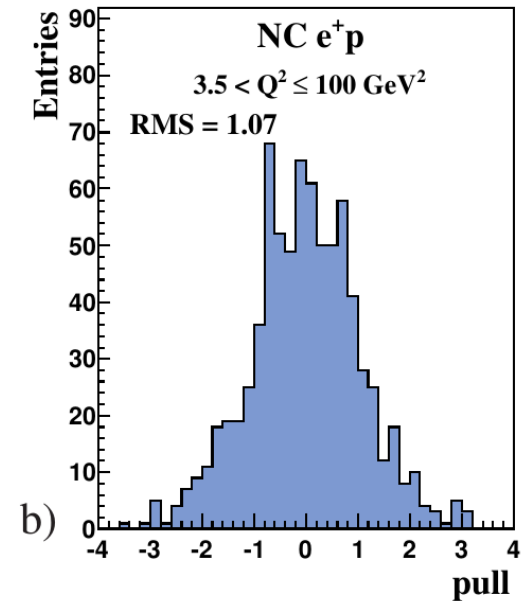
Combination results

- χ^2 of combination: 1687 for 1620 degrees of freedom
- Pull values well distributed around zero with RMS ~ 1
- Great confirmation of consistency of datasets !

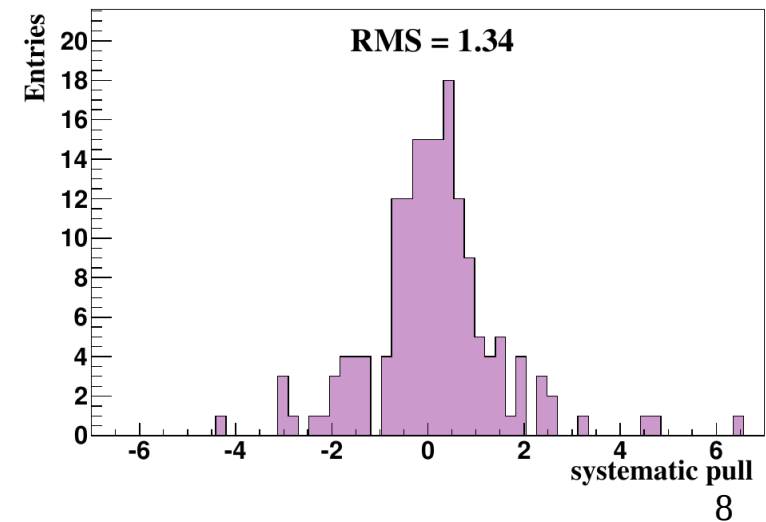
Procedural uncertainties

- Multiplicative vs. additive nature
- Correlation in photoproduction background
- Large pulls in corr. syst. uncert.

$$P^{i,k} = \frac{\mu^{i,k} - \mu^{i,\text{ave}} (1 - \sum_j \gamma_j^{i,k} b_{j,\text{ave}})}{\sqrt{\Delta_{i,k}^2 - \Delta_{i,\text{ave}}^2}}$$



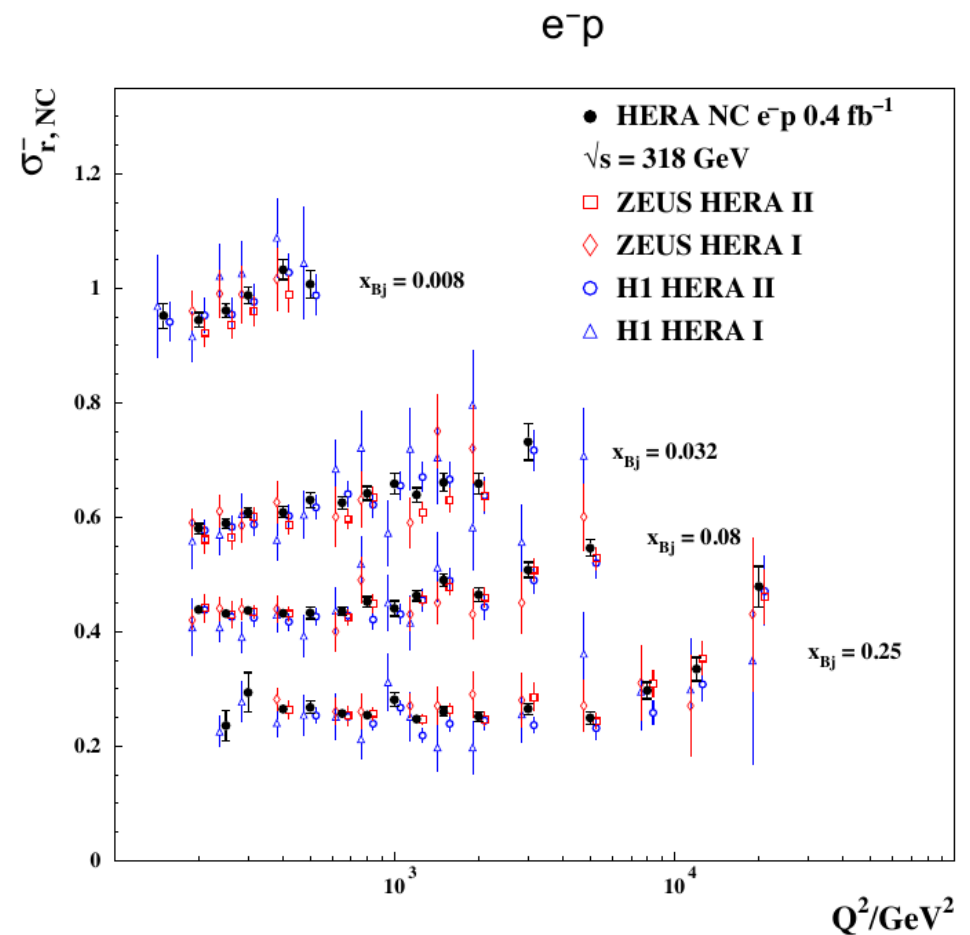
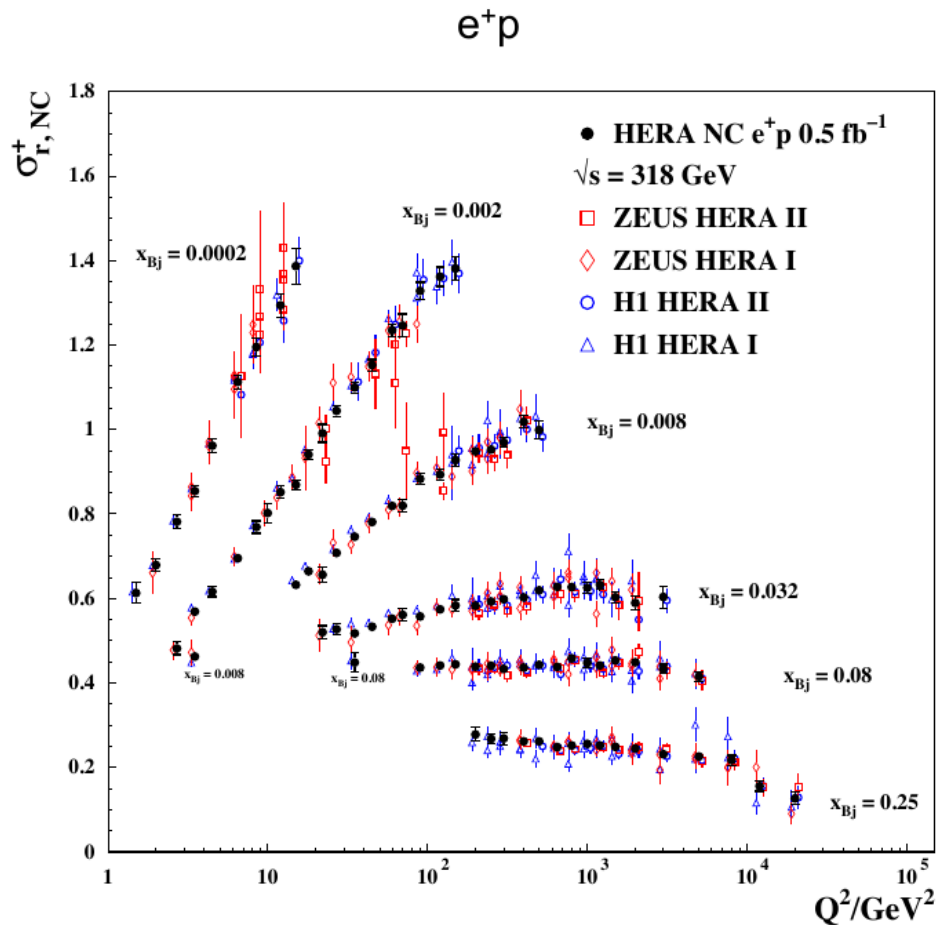
H1 and ZEUS



Combined NC DIS cross sections

Combined HERA data based on approx. 1fb⁻¹

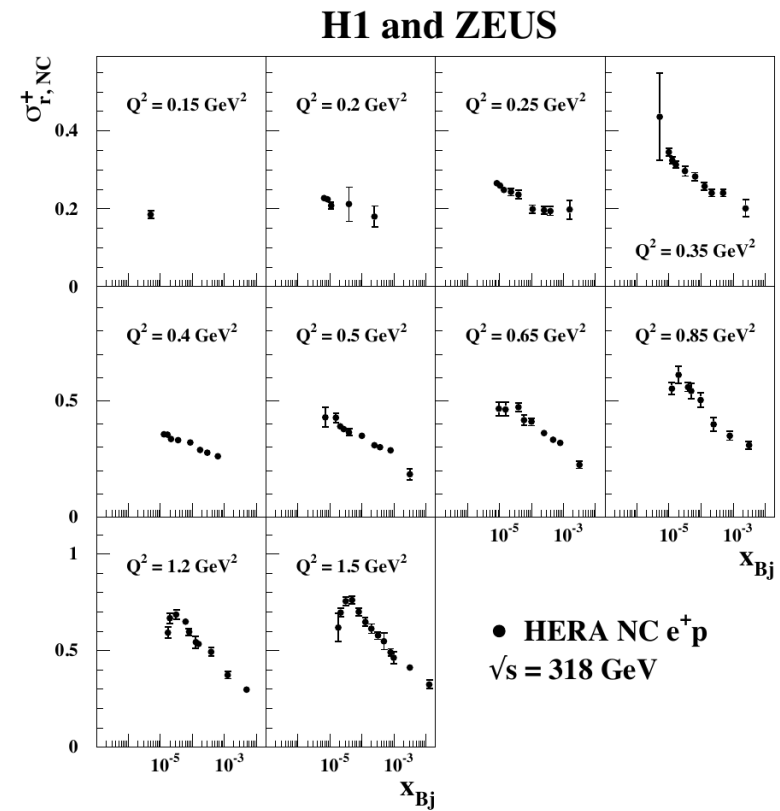
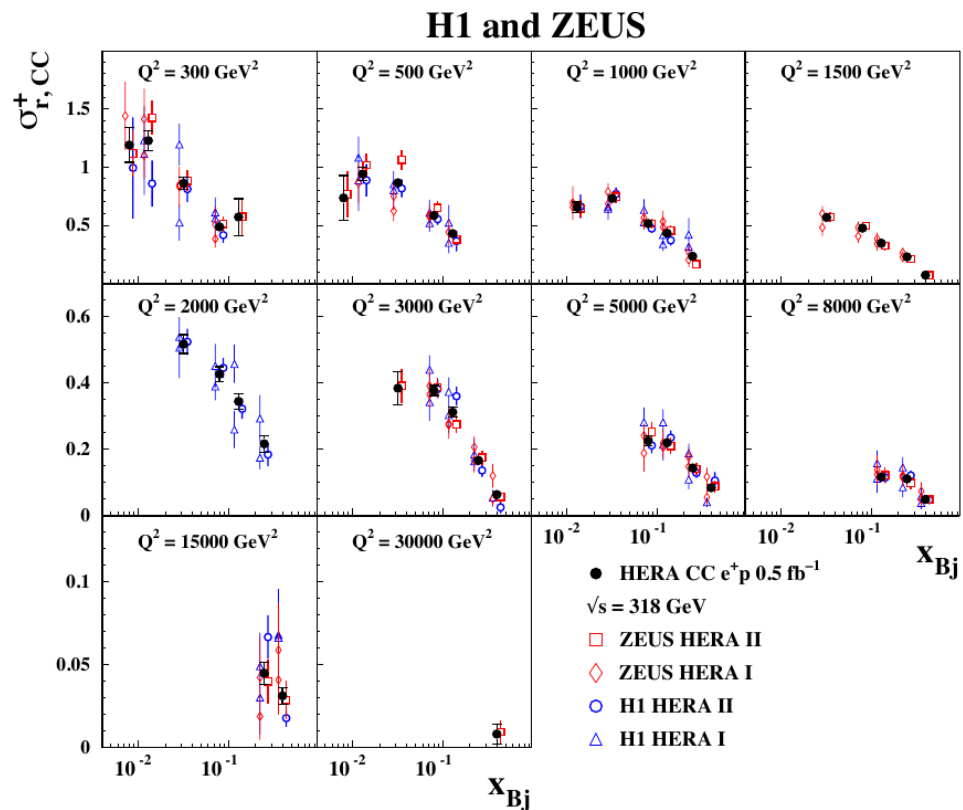
- Only 6 and 4 selected x -bins shown here for $\sqrt{s} = 318$ GeV
- High precision reached over large kinematic range:
Better than 1.3% for $Q^2 < 400$ GeV²



CC DIS and low- Q^2 cross sections

Combined charged current DIS cross sections for $\sqrt{s} = 318$ GeV

- Large improvement in statistical limitations of individual datasets



Further kinematic regions

- Great improvements also for $\sqrt{s} = 225, 251$ and 301 GeV
- Very low- Q^2 and low- x data for $\sqrt{s} = 301$ and 318 GeV
 - $Q^2 > 0.045 \text{ GeV}^2$ and $x_{Bj} > 6 \times 10^{-7}$
 - Interesting for dipole and saturation models

PDF extraction from data: HERAPDF2.0

HERAPDF approach

- Final combined e±p NC and CC data are very precise, so to allow the extraction of the parton densities
- DGLAP Analysis based only on HERA data
- PDFs parameterised at arbitrary starting scale $Q^2_0 = 1.9 \text{ GeV}^2$

xg	xg	$xg(x) = A_g x^{B_g} (1-x)^{C_g} - A'_g x^{B'_g} (1-x)^{C'_g}$	
xu_v	$xU = xu + xc$	$xu_v(x) = A_{u_v} x^{B_{u_v}} (1-x)^{C_{u_v}} (1 + E_{u_v} x^2)$	
xd_v	$xD = xd + xs$	$xd_v(x) = A_{d_v} x^{B_{d_v}} (1-x)^{C_{d_v}}$	<div style="display: flex; align-items: center; margin-bottom: 5px;"> <div style="width: 15px; height: 15px; background-color: #cccccc; margin-right: 5px;"></div> fixed or constrained by sum-rules </div> <div style="display: flex; align-items: center;"> <div style="width: 15px; height: 15px; background-color: #6699cc; margin-right: 5px;"></div> parameters set equal but free </div>
$x\bar{U}$	$x\bar{U} = x\bar{u} + x\bar{c}$	$x\bar{U}(x) = A_{\bar{U}} x^{B_{\bar{U}}} (1-x)^{C_{\bar{U}}} (1 + D_{\bar{U}} x)$	
$x\bar{D}$	$x\bar{D} = x\bar{d} + x\bar{s}$	$x\bar{D}(x) = A_{\bar{D}} x^{B_{\bar{D}}} (1-x)^{C_{\bar{D}}}$	

Minimise χ^2 function with respect to PDF parameters

- Perturbative QCD evolution allows PDFs to be determined at any other scale Q^2
- Calculate theory cross section at given x, Q^2 of measurement
- Usage of momentum/counting sumrules help to constrain parameter space

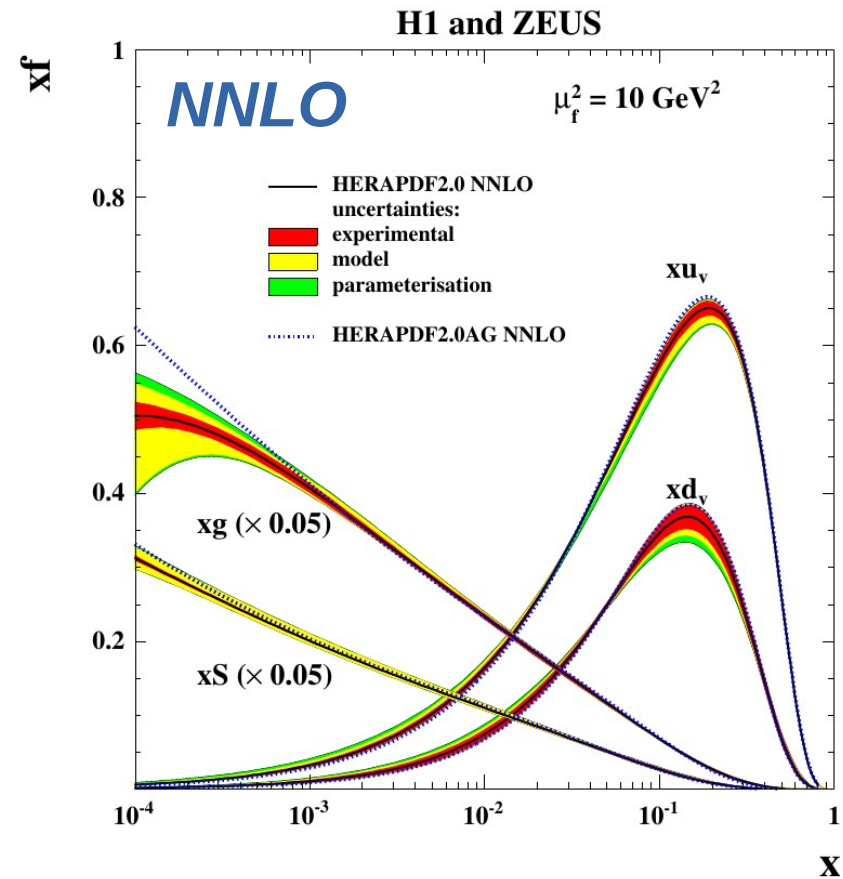
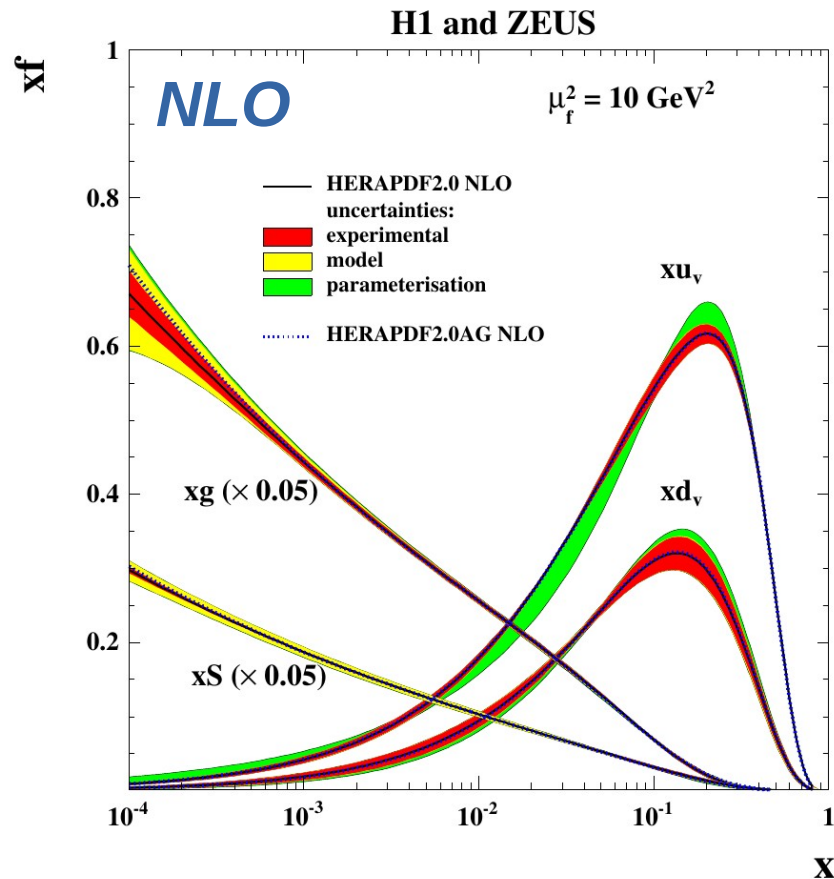
The use of a single consistent data sample allows a more rigorous treatment of the experimental uncertainties

- No fixed target data, therefore no need for heavy-target/deuterium corrections

HERAPDF2.0 NLO and NNLO

Fits performed in LO, NLO and NNLO

- NLO: $\chi^2/\text{ndf} = 1357 / 1131$
- NNLO: $\chi^2/\text{ndf} = 1363 / 1131$



Differences between NLO and NNLO fit

- gluon ceases to raise at low-x
- sea at low-x somewhat steeper w.r.t. NLO

HERAPDF2.0 uncertainties

Experimental Uncertainties

Hessian method uses 14 eigenvector pairs
Standard definition $\Delta\chi^2=1$ for 68% CL error bands

Model Assumptions

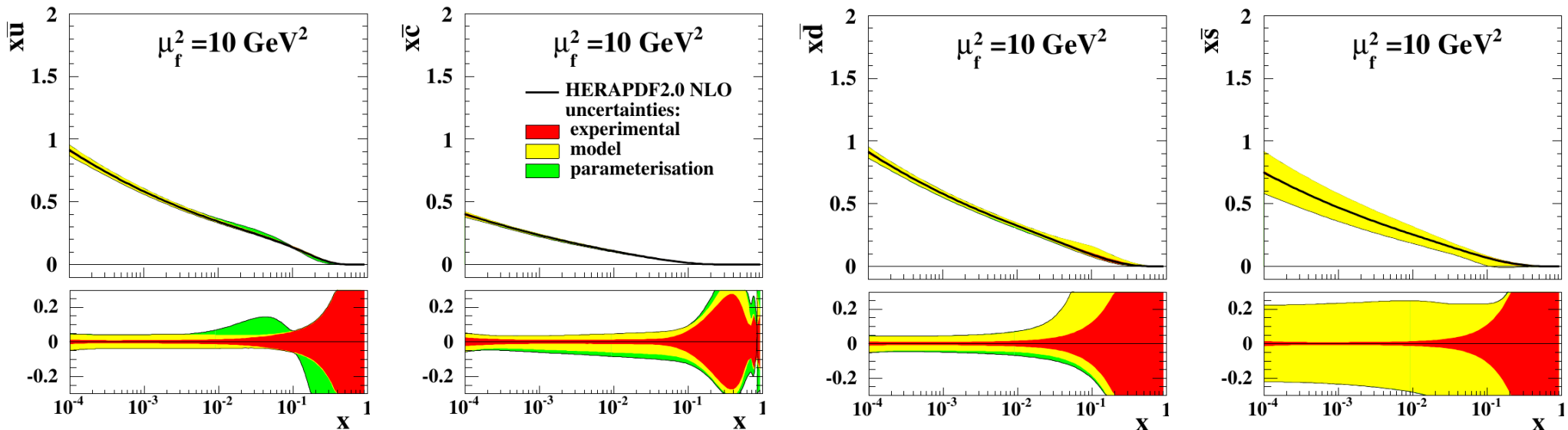
Variation of charm and bottom quark masses M_c , M_b
Variation of Q^2 minimum cut used on input data Q_{\min}^2
Variation of strange quark fraction f_s

Parameterisation Uncertainties

Variation of Q_0^2
Variation of fit using additional 15th parameter

Variation	Standard Value	Lower Limit	Upper Limit
Q_{\min}^2 [GeV ²]	3.5	2.5	5.0
Q_{\min}^2 [GeV ²] HiQ2	10.0	7.5	12.5
M_c (NLO) [GeV]	1.47	1.41	1.53
M_c (NNLO) [GeV]	1.43	1.37	1.49
M_b [GeV]	4.5	4.25	4.75
f_s	0.4	0.3	0.5
$\alpha_s(M_Z^2)$	0.118	–	–
μ_{f_0} [GeV]	1.9	1.6	2.2

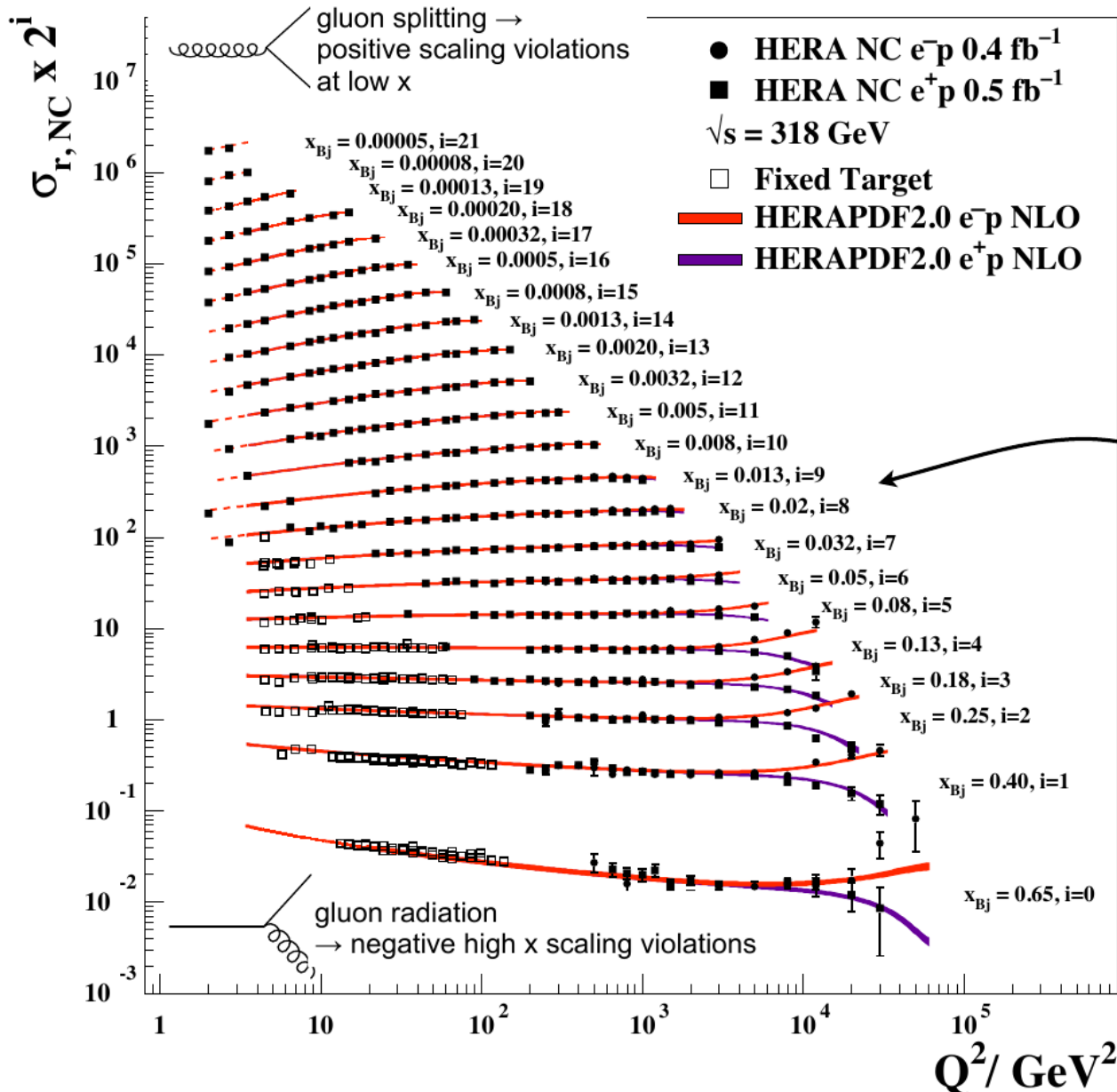
$\alpha_s(M_Z)$ fixed but series of PDFs provided for large range: 0.110 to 0.130



Flavor breakdown of sea distribution

NC cross sections & HERAPDF2.0

Neutral Current $e^\pm p$



Precision 1.3% for $Q^2 < 400 \text{ GeV}^2$
 \Rightarrow factor 2 reduction in error wrt HERA-I

Statistics limited at higher Q^2 and high x

Extended reach at high x compared to H1 preliminary data

This x region is the 'sweet spot'
 High precision with long Q^2 lever arm
 x -range relevant for Higgs production

Combination of high Q^2 data
 HERA-1 and HERA-II

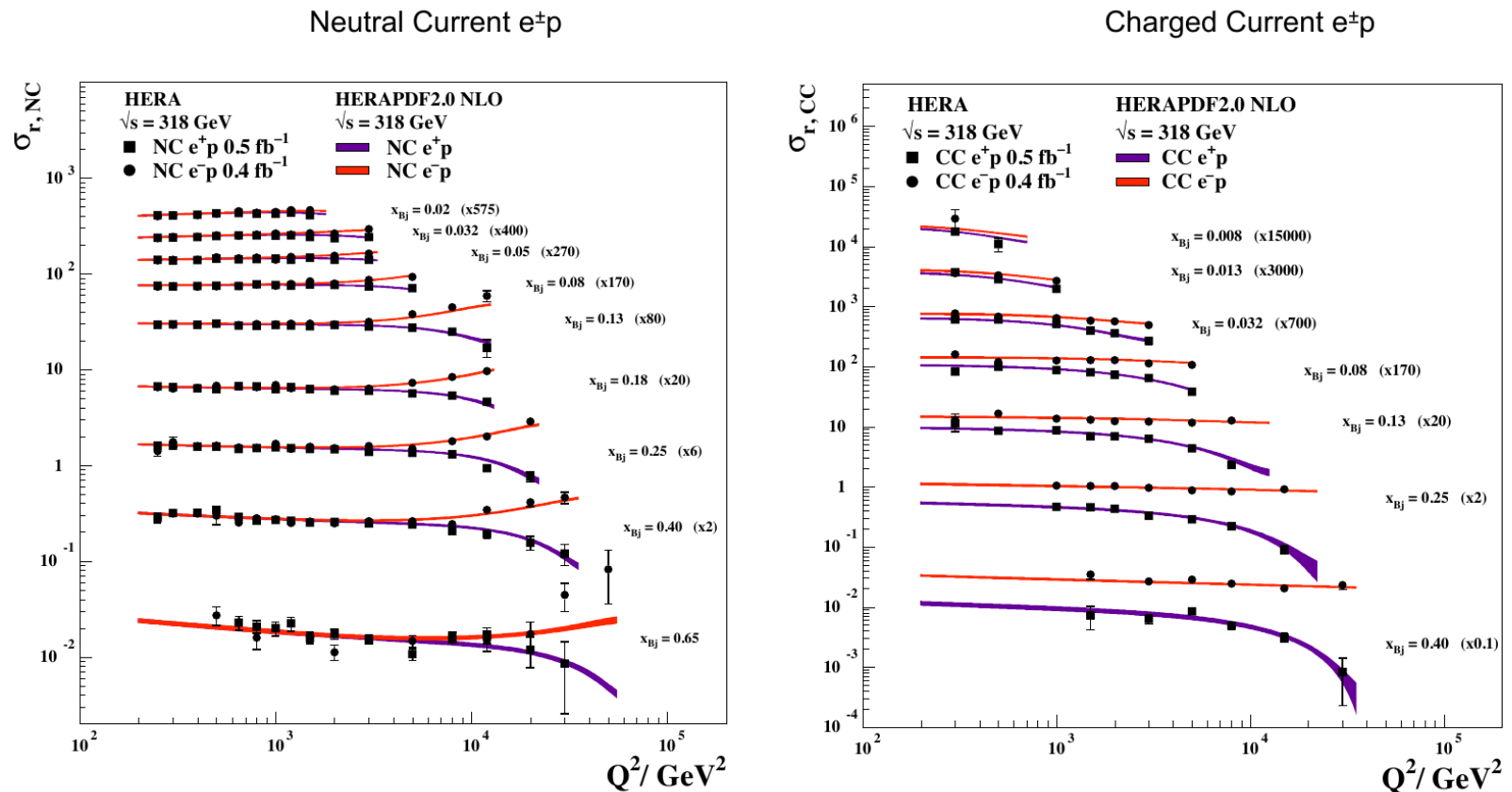
Larger HERA-II luminosity
 \rightarrow improved precision at high x / Q^2

HERAPDF2.0 provides good description

High Q^2 NC & CC Cross Sections

High Q^2 , high- x cross sections

- Difference in NC at high- x for e^+ and e^- due to $x F_3$ and Z-boson exchange
- CC e^+p suppressed at high- x due to $(1-y)^2$ helicity suppression of quarks
- CC e^-p unaffected as helicity suppression applies to anti-quarks



HERAPDF2.0 describes high- x data well for both NC and CC channels

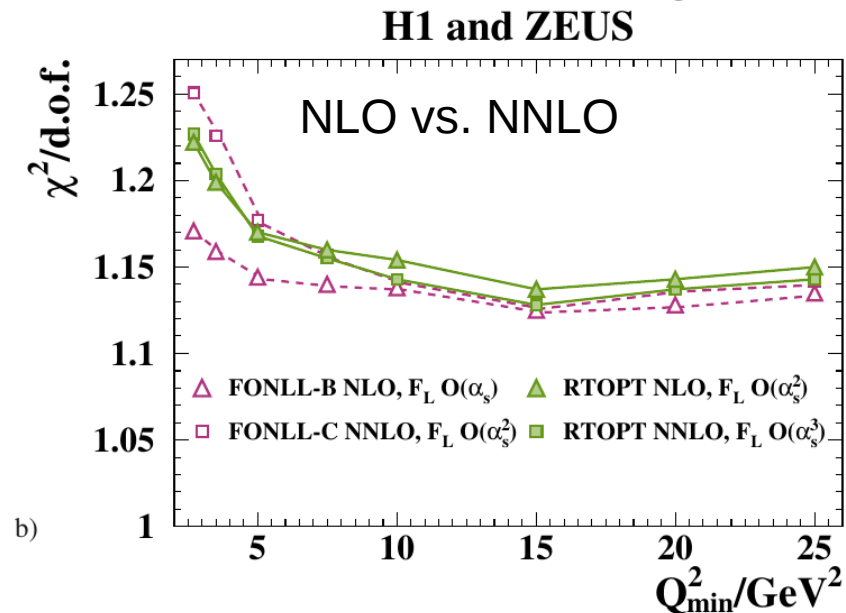
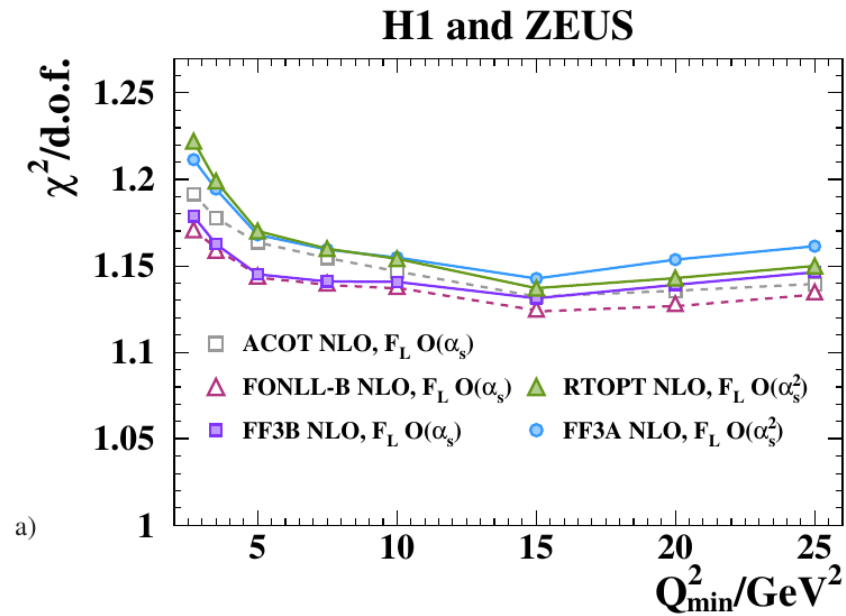
χ^2 and Q^2_{\min} study and heavy flavors

Minimum value of Q^2 for data to ensure that pQCD is applicable

- HERAPDF2.0: $Q^2_{\min} = 3.5 \text{ GeV}^2$
- Consider variation of this cut:
 χ^2 decreases with increase of Q^2
- NLO and NNLO behave similarly
- Low- Q^2 cuts also removes low-x region:
Region where non-pert. effects, $\ln(1/x)$ -resummation, saturation become important
- Fits for $Q^2_{\min} = 10 \text{ GeV}^2$ also released as PDF tables

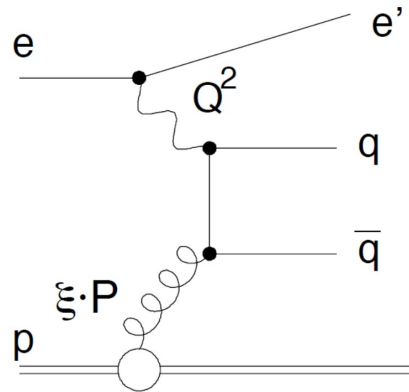
Heavy flavor scheme

- Treating F_L to $O(\alpha_s)$ (the same order as F_2) yields better χ^2 than treating F_L to $O(\alpha_s^2)$
- RT-Opt NNLO is marginally worse than NLO
- FONLL NNLO is worse than NLO

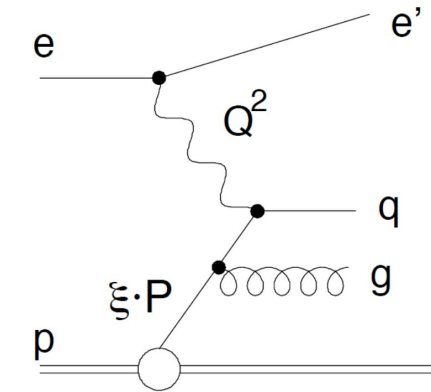


Jet production in DIS

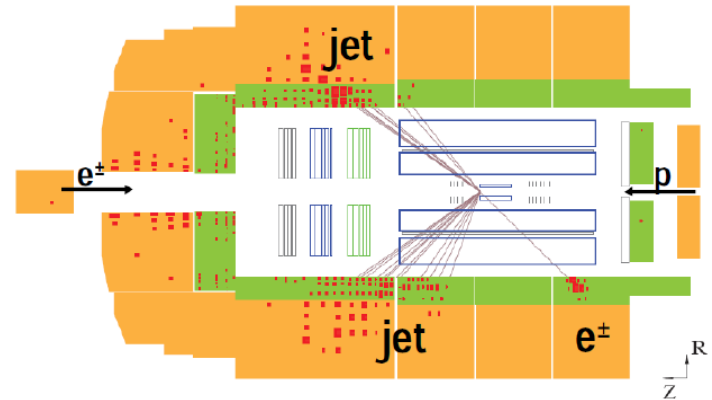
Jet production in leading-order pQCD



boson-gluon fusion



QCD Compton scattering



Jet measurements are performed in Breit-frame

virtual boson collides head on with a parton from the proton

Inclusive jets

Count each jet of an event

Dijet and trijet

Count events with two/three jet event structure

Observable: average transverse momentum of two/three jets

Normalised jets

Normalise all jet data w.r.t. inclusive NC DIS cross section

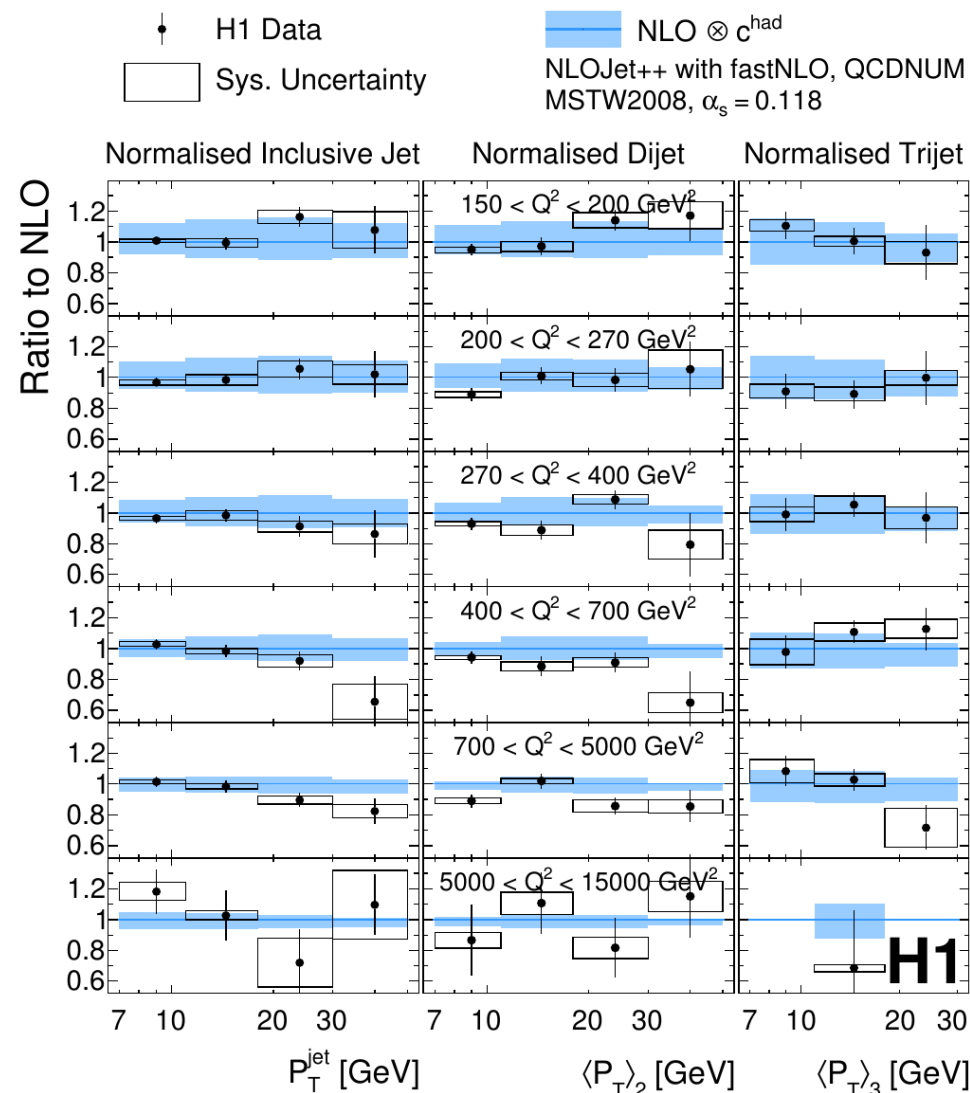
Jet production in DIS

Normalised and non-normalised jet data

- Data well described by NLO theory (nlojet++)
- Data in general with smaller uncertainties than NLO from scale variations
- Differences between different PDF sets typically small

Data used to extract strong coupling constant

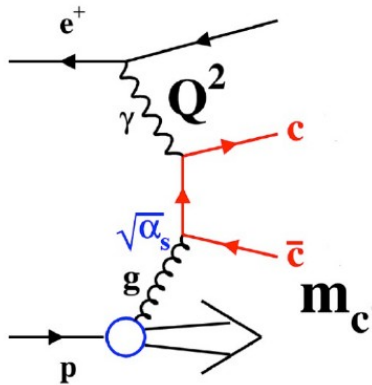
- χ^2 minimisation of α_s in coefficient function
- Dependencies of the PDF on α_s considered as uncertainties



$$\alpha_s(M_Z)|_{k_T} = 0.1165 \quad (8)_{\text{exp}} \quad (5)_{\text{PDF}} \quad (7)_{\text{PDFset}} \quad (3)_{\text{PDF}(\alpha_s)} \quad (8)_{\text{had}} \quad (36)_{\mu_r} \quad (5)_{\mu_f}$$

$$= 0.1165 \quad (8)_{\text{exp}} \quad (38)_{\text{pdf,theo}} \cdot$$

Charm production in DIS

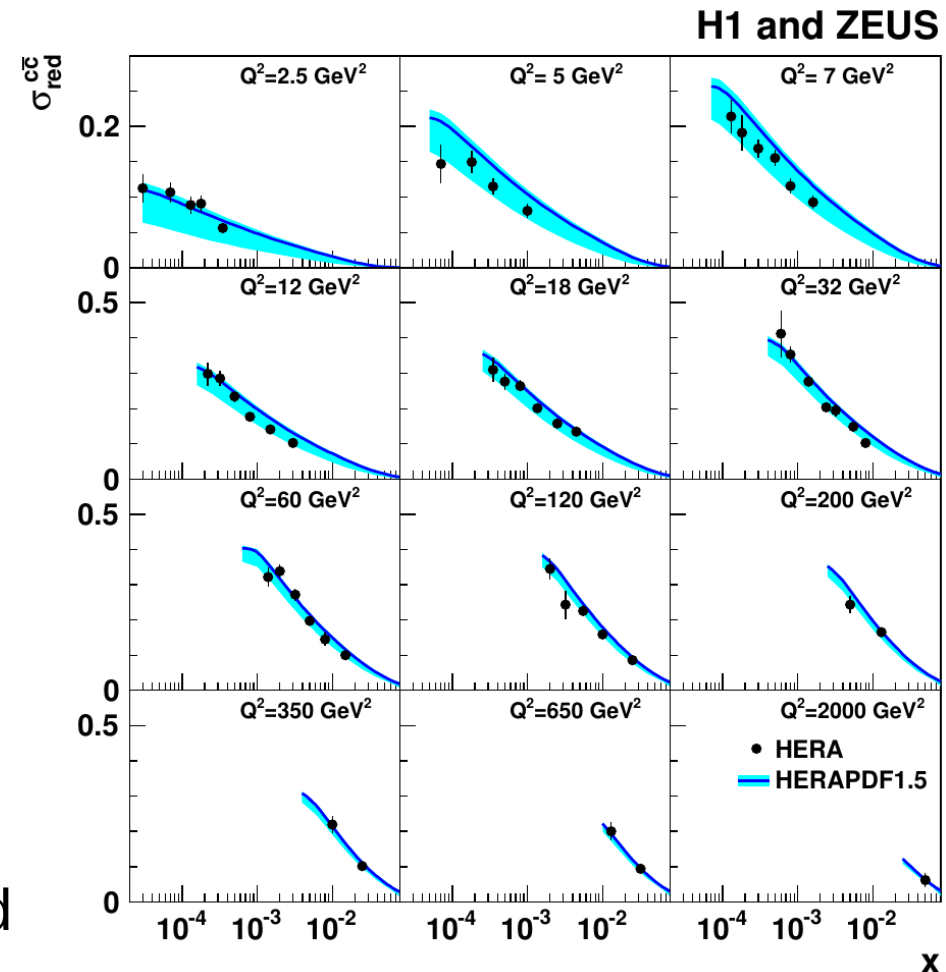


Charm production at HERA

- Charm is produced in virtual photon-gluon fusion
- Charm production directly sensitive to the gluon density $xg(x)$

Combined charm cross sections

- Wealth of HERA charm data combined into common charm cross sections



$$\frac{d^2\sigma^{c\bar{c}}}{dx dQ^2} = \frac{2\pi\alpha^2(Q^2)}{xQ^4} ([1 + (1 - y)^2] F_2^{c\bar{c}}(x, Q^2) - y^2 F_L^{c\bar{c}}(x, Q^2))$$

Extraction of charm mass running

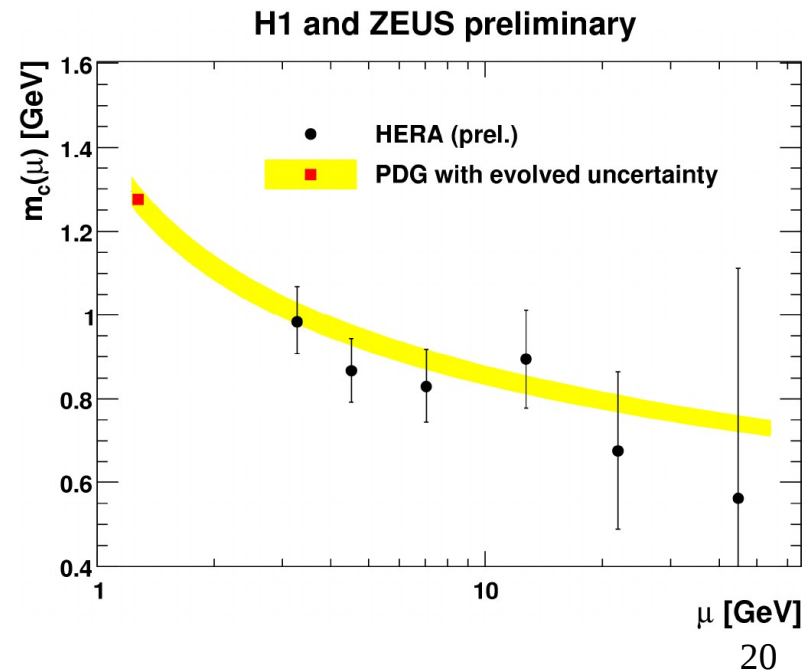
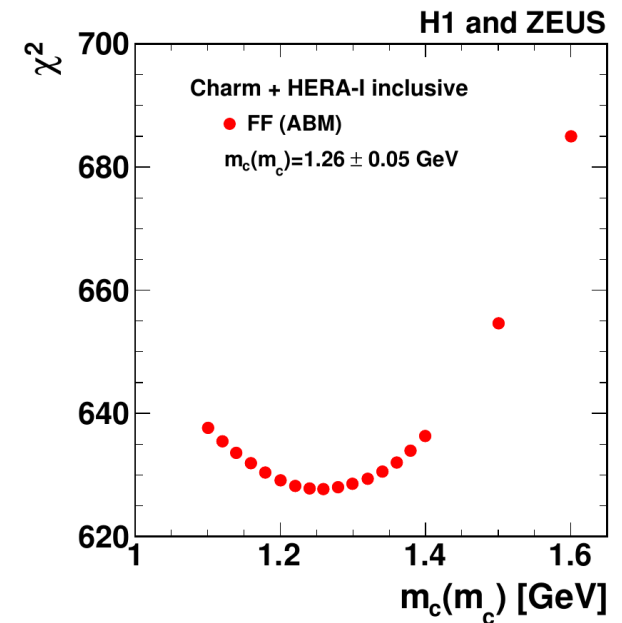
Extraction of charm mass

- Simultaneous fit of combined charm data + inclusive HERA-I DIS data
- Different heavy-flavor schemes explored
- FFNS ABM scheme defines charm mass in $\overline{\text{MS}}$ scheme

$$m_c(m_c) = 1.26 \pm 0.05_{\text{exp}} \pm 0.03_{\text{mod}} \pm 0.02_{\text{par}} \pm 0.02_{\text{as}} \text{ GeV}$$

Charm mass running

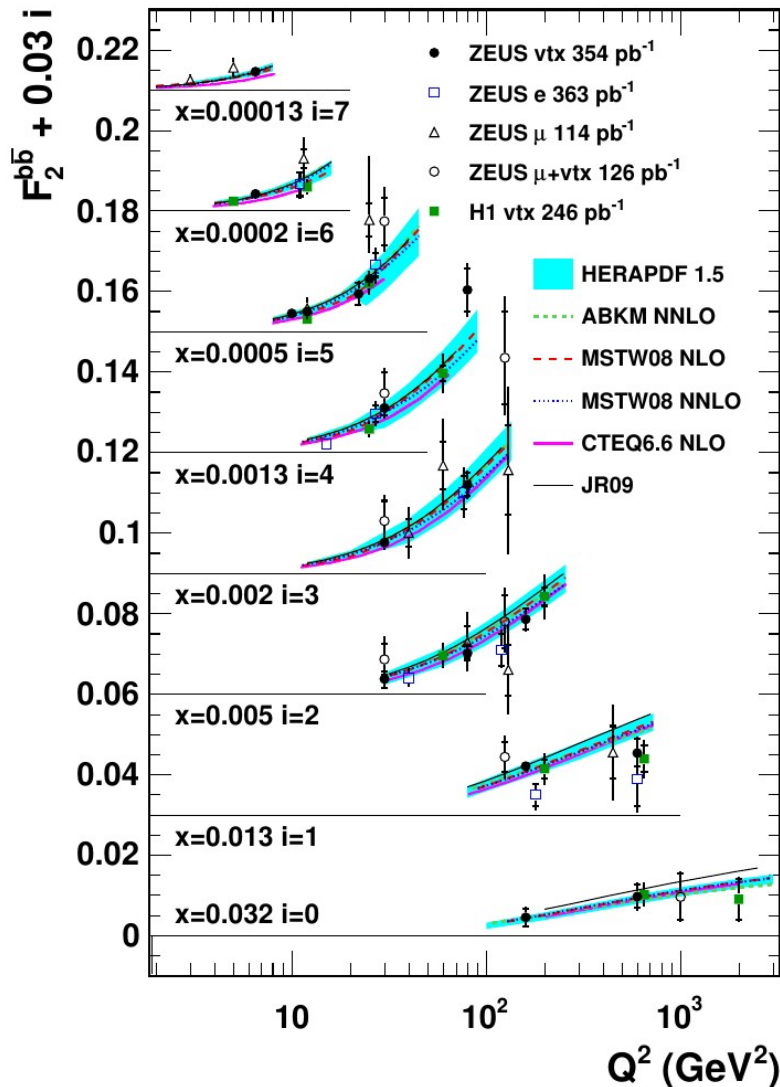
- extract $m_c(m_c)$ separately for 6 kinematic ranges in $\mu^2 = Q^2 + 4m_c^2$
- use appropriate PDF set for each mass (from inclusive DIS data only)
- fit charm data + HERA-I incl. data
- Translate back to $m_c(\mu)$ using LO formula consistent with NLO $\overline{\text{MS}}$ QCD fit (OpenQCDrad, Alekhin et al.)



Determination of beauty mass

Beauty cross sections

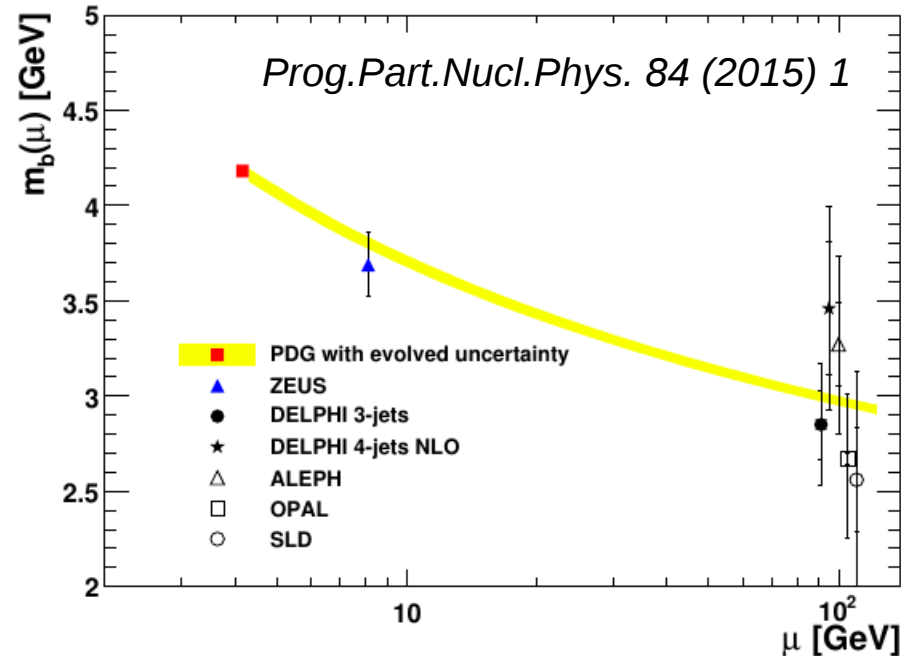
- Measured of HF jets using secondary vertices + lifetime tag
- Good description of data by massive NLO QCD predictions



Extraction of b-quark mass

- QCD fit (FFNS) of HERA-I incl. data + ZEUS beauty data
- m_b as free parameter

$$m_b(m_b) = 4.07 \pm 0.14 \text{ (fit)}^{+0.01}_{-0.07} \text{ (mod.)}^{+0.05}_{-0.00} \text{ (param.)}^{+0.08}_{-0.05} \text{ (theo.) GeV}$$

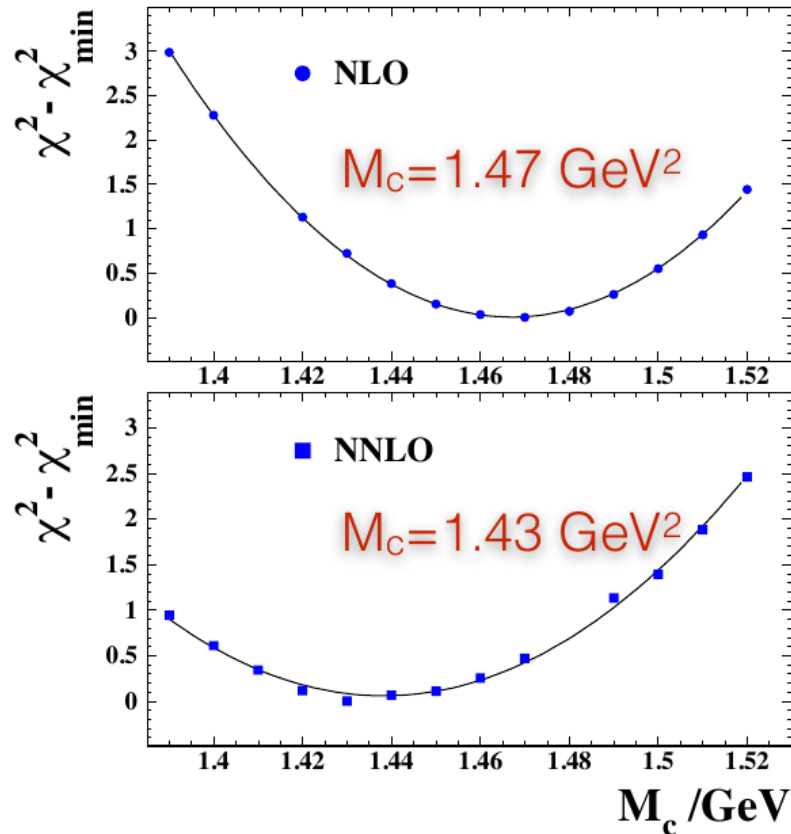


Charm and jet data in HERAPDF2.0

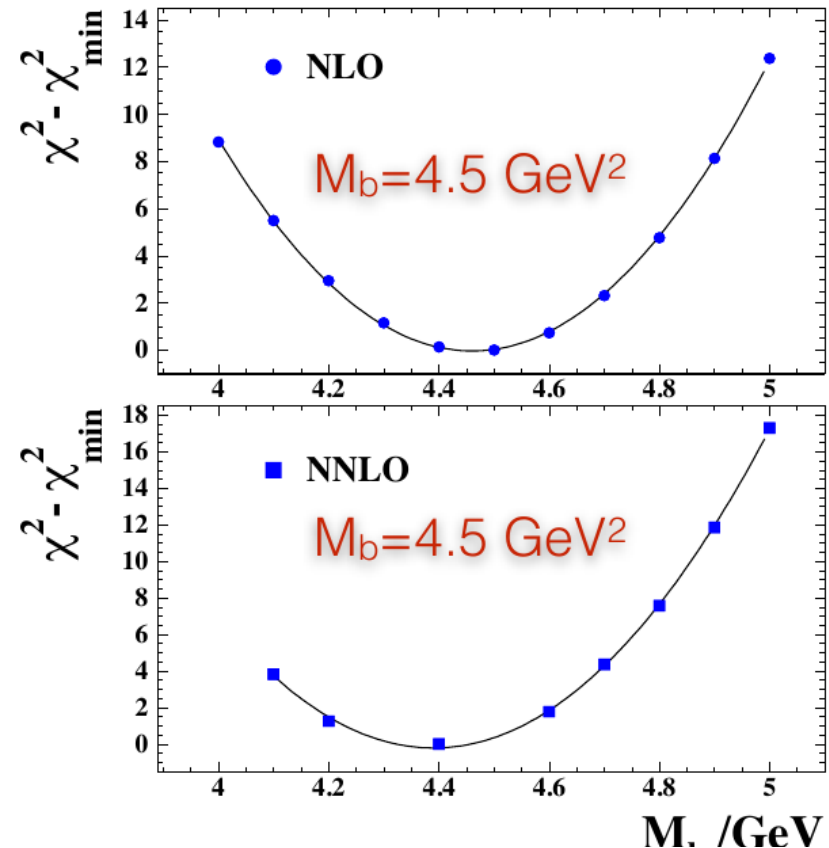
Charm and bottom data used in HERAPDF2.0 QCD analysis

- Charm and bottom data used to determine best quark-mass parameters
- Values of charm and bottom masses used DGLAP fits determined as χ^2 scan of NLO and NNLO fits

H1 and ZEUS



H1 and ZEUS



Charm and jet data in HERAPDF2.0

Additional datasets in QCD analysis

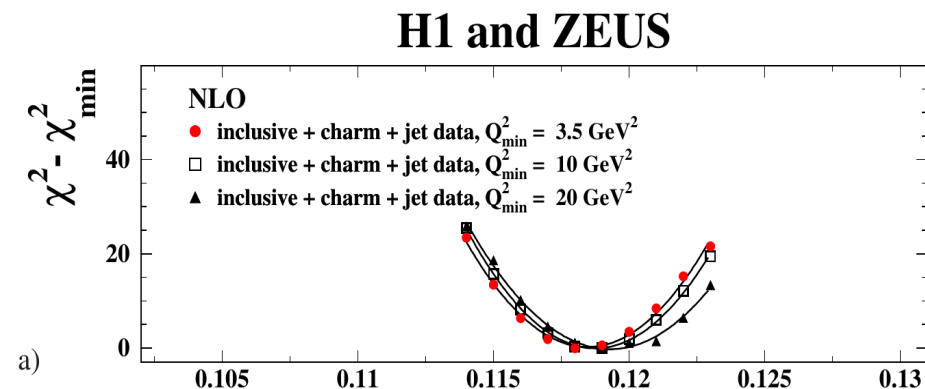
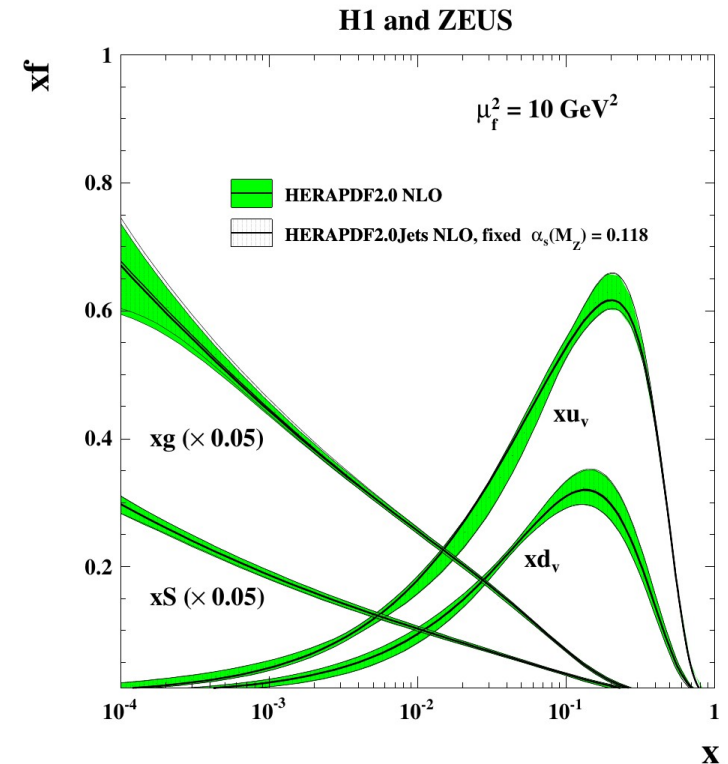
- Combined charm cross sections
- H1 norm. multijets at high Q^2 (HERA-II)
- H1 multijets at low Q^2 (HERA-I)
- H1 incl. jets at high Q^2 (HERA-I)
- ZEUS dijets at high Q^2 (HERA-II)
- ZEUS incl. jets at high Q^2 (HERA-I)
- Jet predictions available in NLO (nlojet++)
- Jet data significantly helps to disentangle gluon- α_s correlation

Determination of strong coupling

- α_s is additional free parameter in PDF fit
- Jet data constrain α_s

$$\alpha_s(m_Z) = 0.1183 \pm 0.0009_{\text{exp}} \pm 0.0005_{\text{mod}} \pm 0.0012_{\text{had}} \pm 0.004_{\text{scale}}$$

- Value mostly constrained by H1 norm. multijet data



Usage of HERA 'combined' data

HERA combined data

- Limit on effective quark radius
- Consider finite radius through form-factor

$$\frac{d\sigma}{dQ^2} = \frac{d\sigma^{\text{SM}}}{dQ^2} \left(1 - \frac{R_e^2}{6} Q^2\right)^2 \left(1 - \frac{R_q^2}{6} Q^2\right)^2$$

- Fit PDFs and 'quark radius'
- 95% C.L. on quark radius

$$-(0.47 \cdot 10^{-16} \text{ cm})^2 < R_q^2 < (0.43 \cdot 10^{-16} \text{ cm})^2$$

Data improves previous limit by ZEUS and H1 which has also previously constrained

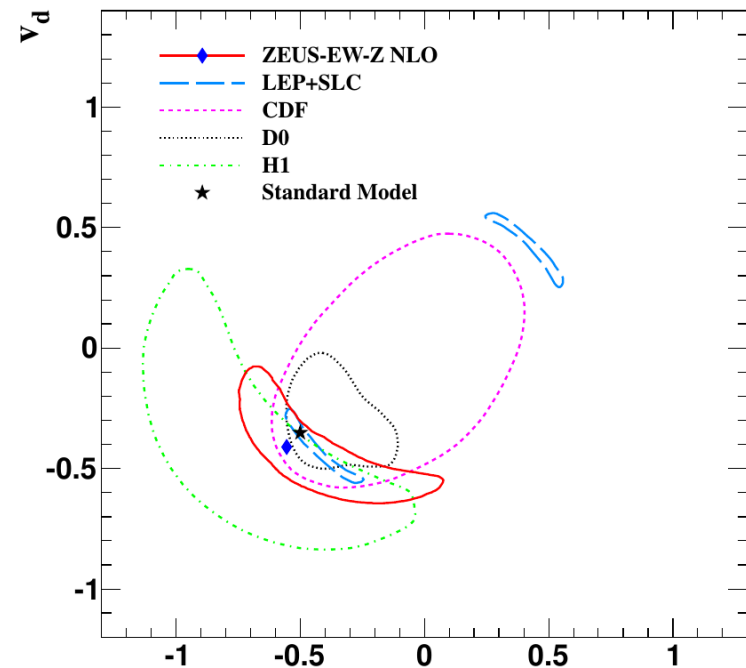
- Limits on compositeness scale of contact interactions (3.6 – 7.2 TeV)
- Limits on low-scale quantum gravity gravitons
- Limits on Leptoquark exchange and s-quarks

H1 and ZEUS data + ZEUS polarized HERA-II data

- Study Couplings of u- and d-quarks to Z-boson
- Use in additional ZEUS polarized data

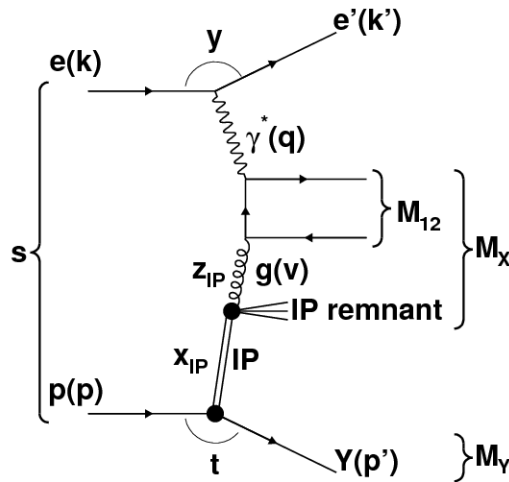
$$\tilde{F}_2^\pm = F_2^\gamma - (v_e \pm P_e a_e) \chi_Z F_2^{\gamma Z} + (v_e^2 + a_e^2 \pm 2P_e v_e a_e) \chi_Z^2 F_2^Z,$$

- Simultaneous fit of PDFs and axial and vector-'quark couplings'
- Values consistent with SM expectations
- Sensitivity on u-quark higher than d-quark

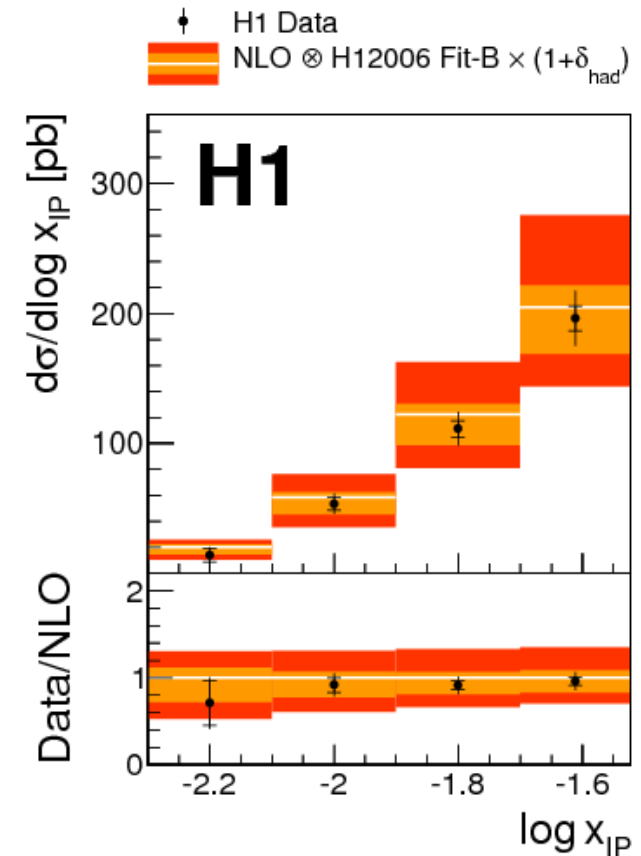


Dijets in diffractive DIS (LRG)

(Inclusive) dijets in diffractive DIS



- Diffractive events identified by 'large rapidity gap' (LRG)
- $4 < Q^2 < 100 \text{ GeV}^2$, $p_{T, \text{jet1(2)}} > 5.5 \text{ (4.0) GeV}$
- Theory: nlojet++ & H1DPDF2006 FitB
- Data used to extract strong coupling constant
 - > Fit supports concept of pQCD calculations for diff. dijets
 - > Exp. precision overshoots theoretical one



$$\alpha_s(M_Z) = 0.119 \pm 0.004 \text{ (exp)} \pm 0.002 \text{ (had)} \pm 0.005 \text{ (DPDF)} \pm 0.010 (\mu_r) \pm 0.004 (\mu_f)$$

$$= 0.119 \pm 0.004 \text{ (exp)} \pm 0.012 \text{ (DPDF, theo)}$$

Diffr. Dijets in Photoprod. and DIS (VFPS)

History

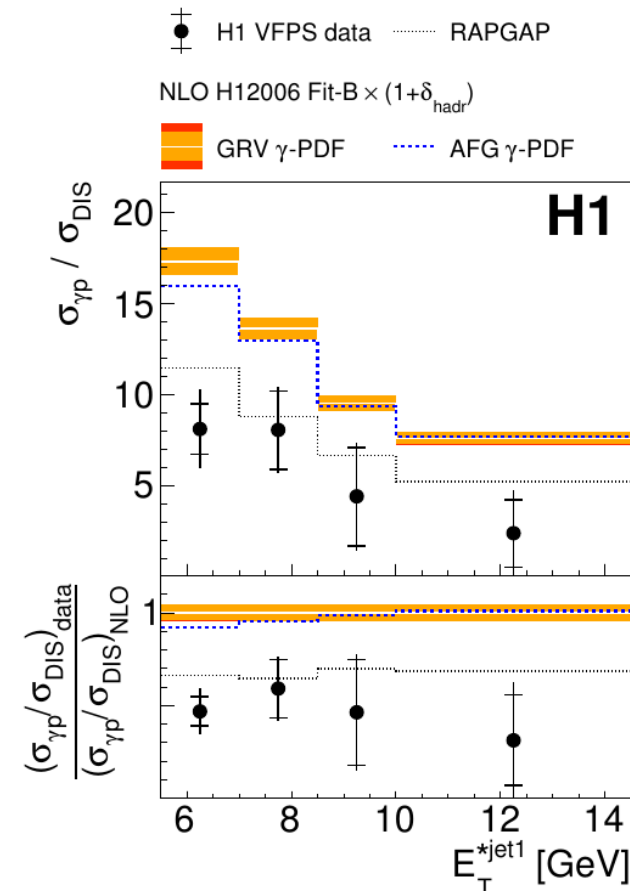
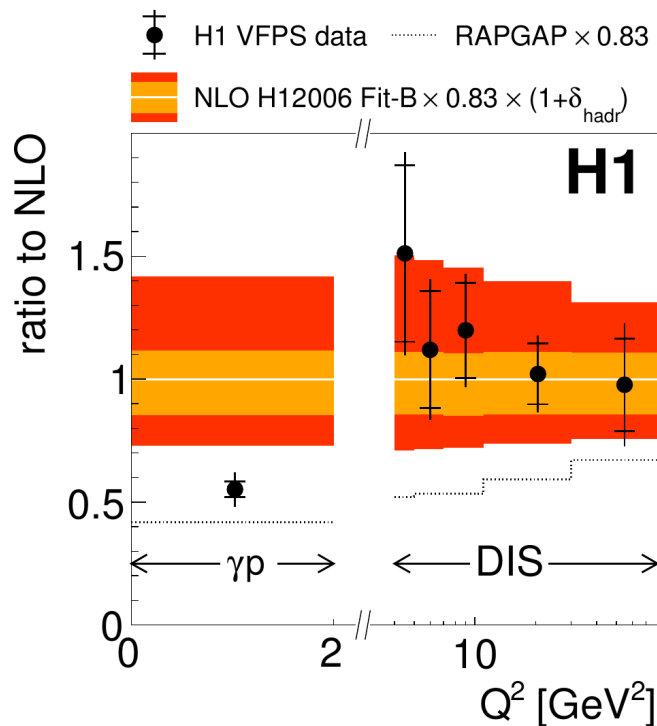
- 'Factorisation breaking' observed in diffractive events at Tevatron
- Photoproduction provides similar testing ground
- Fact. breaking observed by H1 but not by ZEUS

Here: Simultaneous measurement of dijets in diffr. DIS and PHP

- Use VFPS 220m from interaction point
- Calculate double-ratios: PHP/DIS

Single differential cross sections

- DIS data well described by NLO
- PHP NLO overshoots data
- New data with complementary method consistent with previous H1 results
- 'Suppression' shows no dependence as function of x_γ or E_{T}^{jet1}



Study diffractive models

Exclusive dijets in diffractive DIS

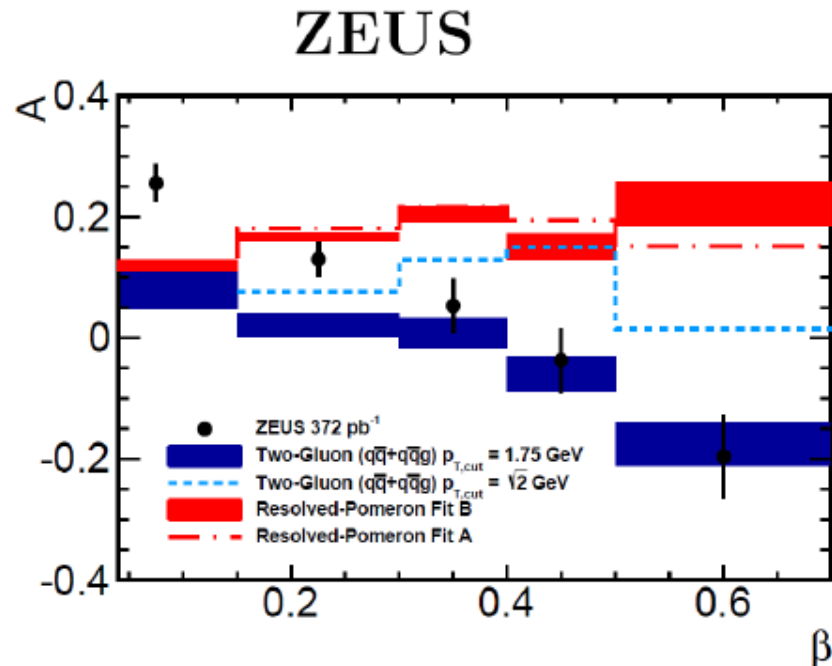
- Study (normalised) angle between jet-plane and lepton-plane

$$\frac{1}{\sigma} \frac{d\sigma}{d\phi} \propto 1 + A \cos 2\phi$$

- Sensitive to nature of diffr. exchange: Resolved pomeron vs. two-gluon exchange model

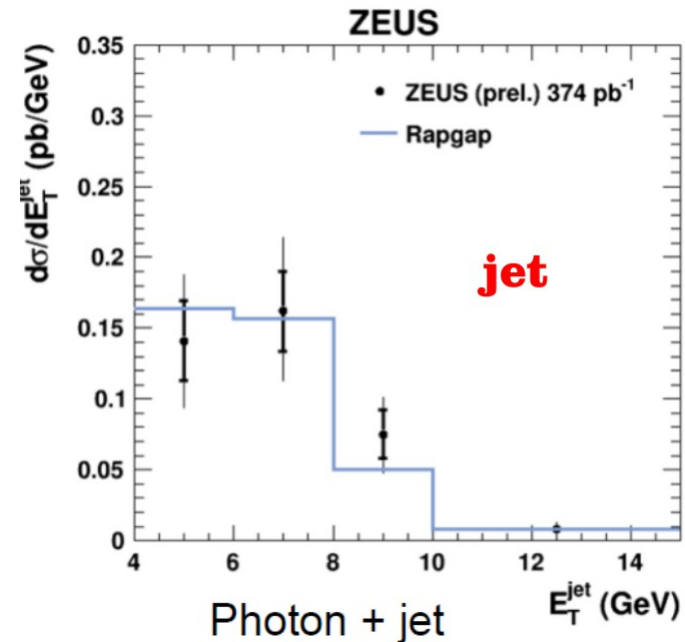
$$\beta = x_{Bj}/x_{IP}$$

- Two-gluon model is more successful in describing data than resolved Pomeron model



Diffractive prompt isolated photons

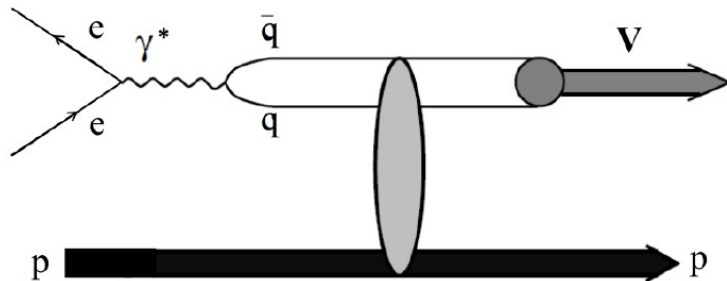
- Analysis extends prompt photon analysis in non-diff. PHP
 - Reminder: NLO and k_T-factorization predictions give good descriptions
- Prompt photon variables well described by Rapgap & H1PDF2006-FitB
- Problems at z_{IP} → 1, where H1PDF2006-FitB was not fitted



Exclusive vector-meson production

Exclusive electroproduction of vector meson

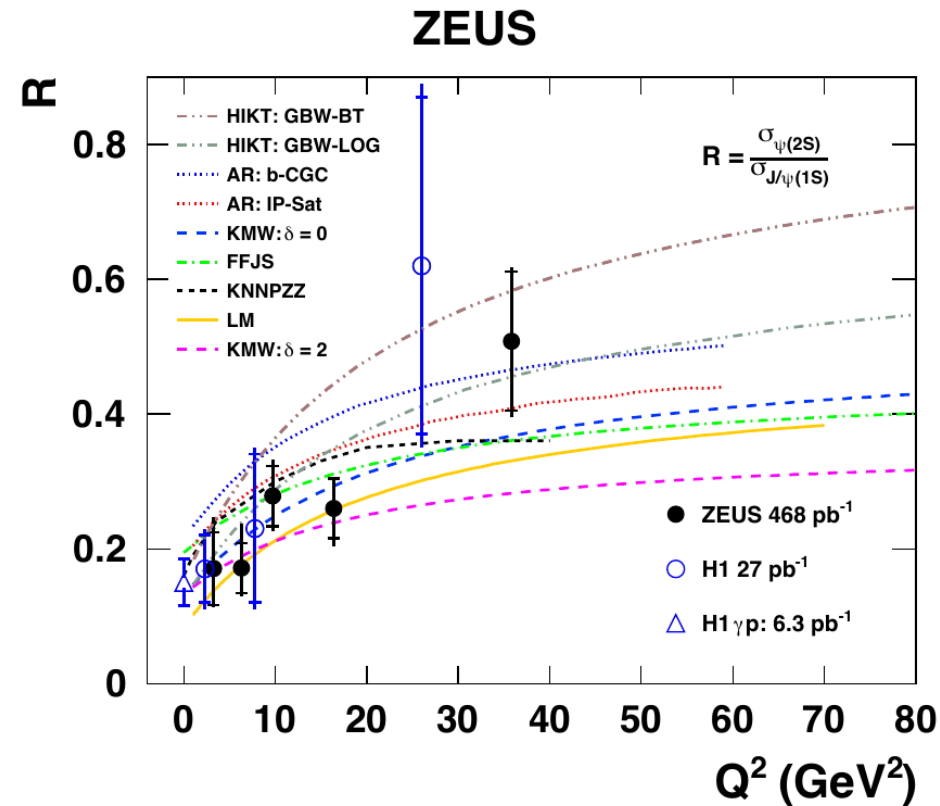
- Measure ratio of $\psi(2s)$ over $J/\psi(1s)$ as function of Q^2



- Identify VM in $\mu^+\mu^-$ decay channels
 - $30 < W < 210$ GeV, $|t| < 1\text{GeV}^2$
- Compare against various models for
 - Generating cc-dipole in photon
 - cc-dipole scattering amplitude
 - Probability to form vector charmonium

All models perform reasonably well

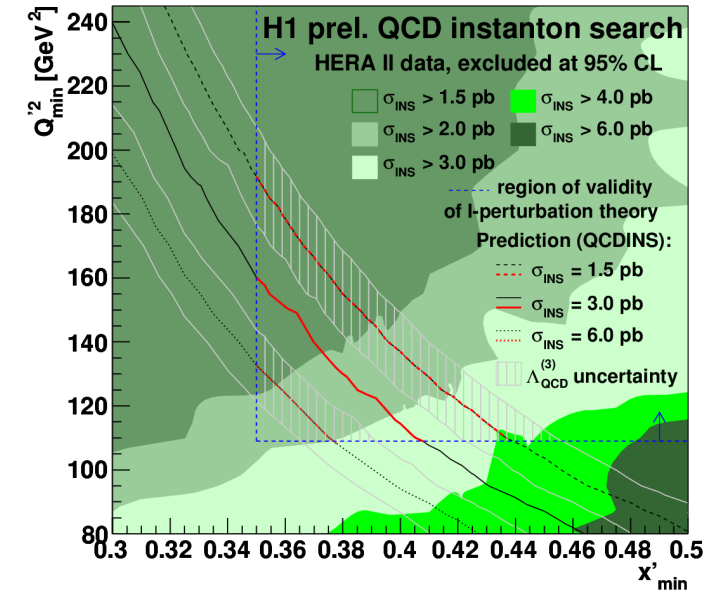
- Ratio tend to be constant vs. W and $|t|$
- Spread indicate large theory uncertainty



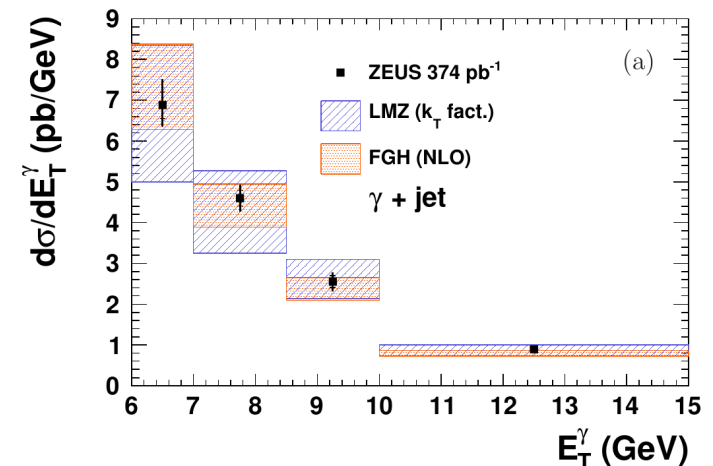
Wealth of more QCD related measurements

New measurements, old measurements, and maybe forgotten ones...

- Search for QCD instantons
to be published by H1
- Isolated photons in photoproduction
PLB 730 C (2014) 293 & JHEP 08 (2014) 03
- Exclusive ρ^0 Meson Photoproduction with a Leading Neutron at HERA
Eur.Phys.J.C76 (2016) 1
- Elastic and Proton-Dissociative Photoproduction of J/psi Mesons at HERA
Eur.Phys.J.C73 (2013) 2466
- Event shapes
Nucl. Phys. B 767 (2007) 1, EPJ C46 (2006) 343
- Numerous D^* measurements
JHEP 1509 (2015) 149, ...
- Charged particle production spectra
Eur.Phys.J.C73 (2013) 2406
-



ZEUS



Conclusion

HERA inclusive DIS cross sections finalized

- One consistent dataset of all HERA structure function data
- HERAPDF2.0 as HERA-only PDF
- Baseline data for future PDF fits

Wealth of precision QCD measurements

Many topics not covered in this short talk

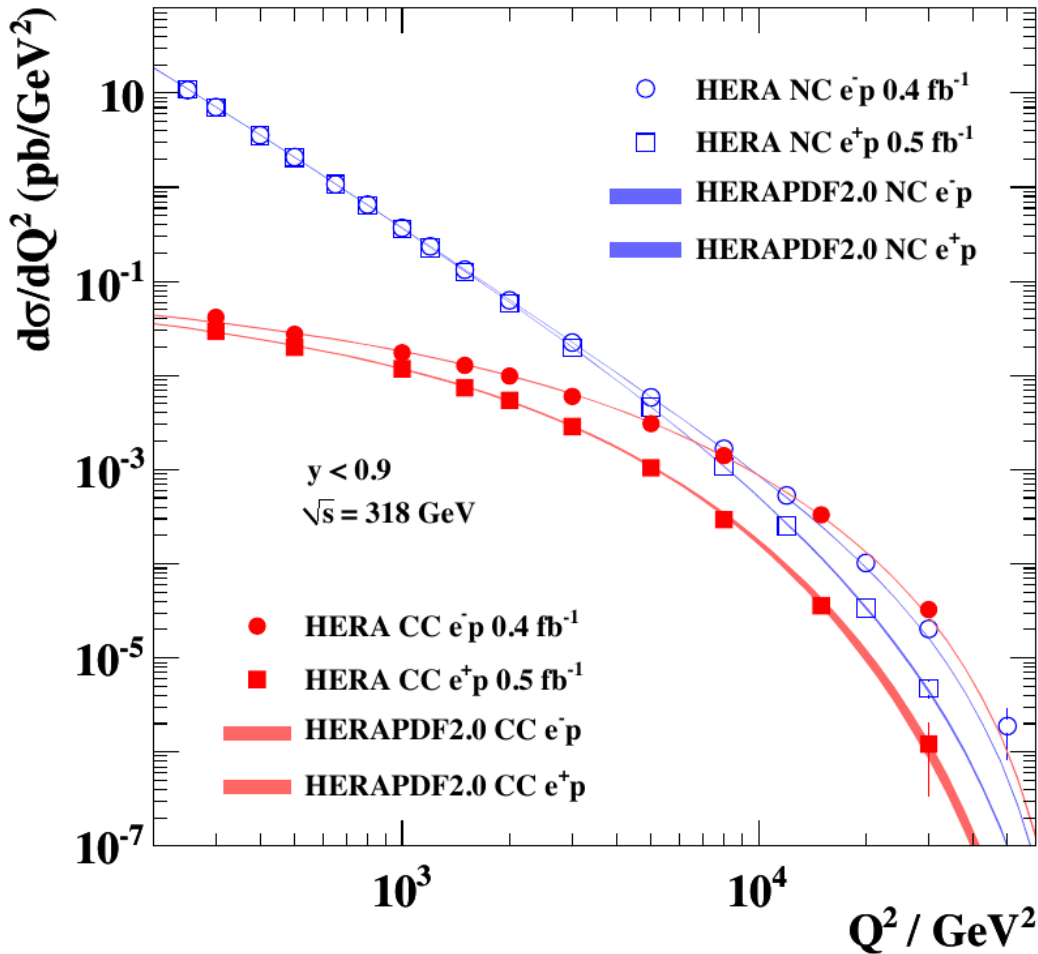
- Jet and photon cross sections
- Various searches and limits
- Strong diffractive DIS programme
- Many exclusive final states measured with full HERA-II statistics
- low-x and soft physics

HERA experiments still active

- Improved/new measurements can still be expected this year

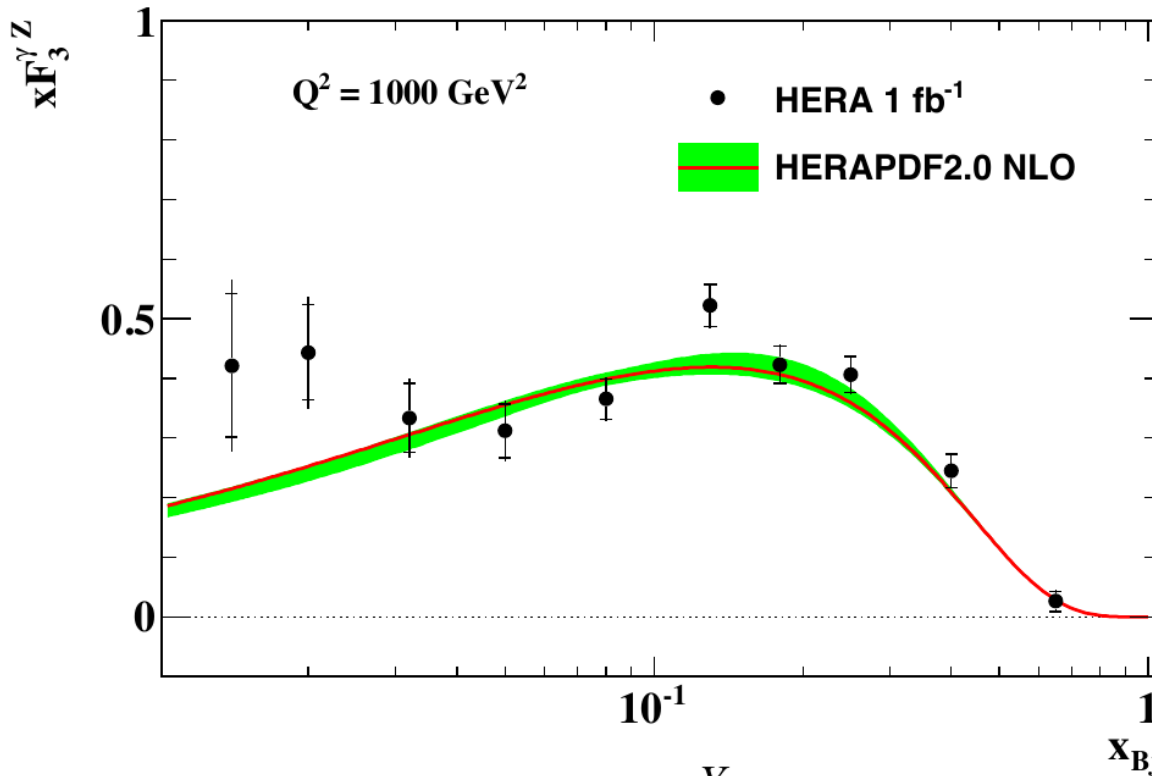
Electroweak symmetry breaking

Electroweak symmetry breaking



- H1 / ZEUS completed their final SF measurements
- New HERA-II data provide tighter constraints at high x / Q^2
- These data provide some of the most stringent constraints on PDFs
- Stress-test of QCD over 4 orders of mag. in Q^2
- DGLAP evolution works very well
- HERA data provide a self-consistent data set for complete flavour decomposition of the proton
- Final combination of HERA data completed
- HERAPDF2.0 QCD fit at NLO & NNLO

Valence quarks and xF3



At high Q^2 xF_3 arises due to Z^0 effects
 enhanced e^- cross section wrt e^+
 Difference is xF_3
 Sensitive to valence PDFs

$$x\tilde{F}_3 = \frac{Y_+}{2Y_-} (\tilde{\sigma}_{NC}^- - \tilde{\sigma}_{NC}^+) \approx a_e \chi_Z xF_3^{\gamma Z}$$

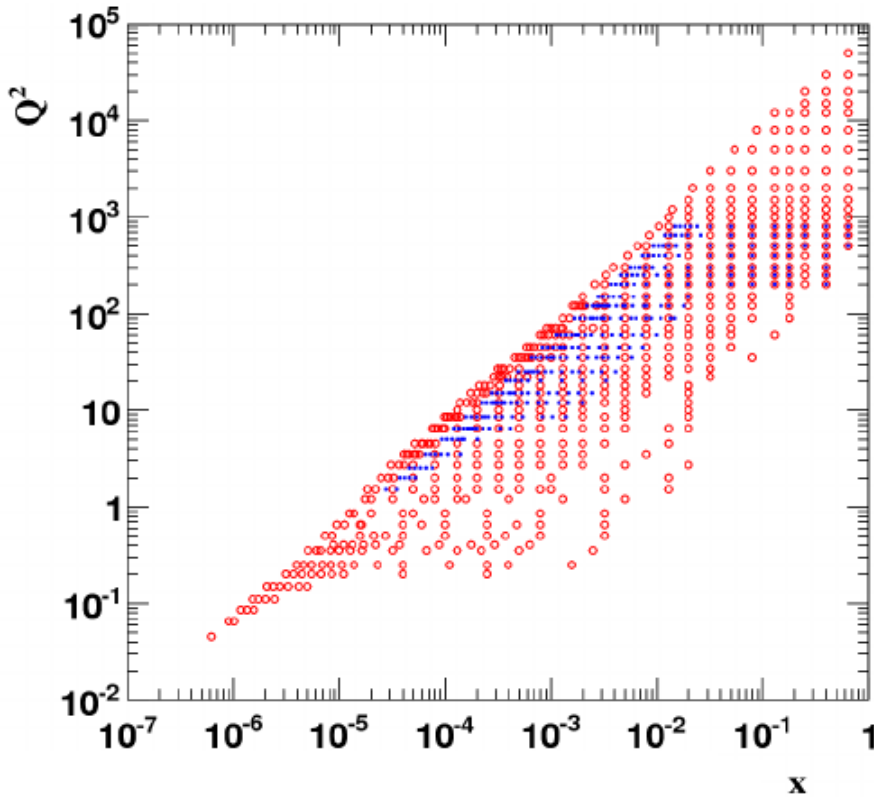
$$x\tilde{F}_3 \propto \sum (xq_i - x\bar{q}_i)$$

Measure integral of $xF_3^{\gamma Z}$ - validate sumrule:

$$\int_{0.016}^{0.725} dx F_3^{\gamma Z}(x, Q^2 = 1500 \text{ GeV}^2) = 1.314 \pm 0.057(\text{stat}) \pm 0.057(\text{syst})$$

LO integral predicted to
 be $5/3 + \mathcal{O}(\alpha_s/\pi)$

'Swimming' of data points



Data are combined onto a common x, Q^2 grid

Two grids used:

inclusive measurements $\sqrt{s}=318$ GeV

fine x grid for $\sqrt{s}=251$ & 225 GeV

2927 data points \rightarrow 1307 combined measurements

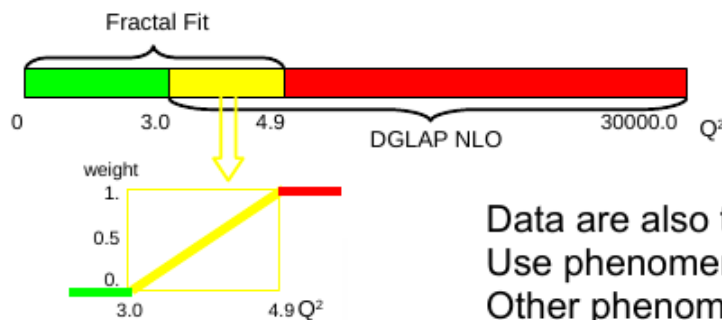
Data are translated to nearest x, Q^2 grid point

Iterative process using NLO QCD fit to data

Use uncombined data in first iteration

Then combined data in later iterations

No changes after 3 iterations



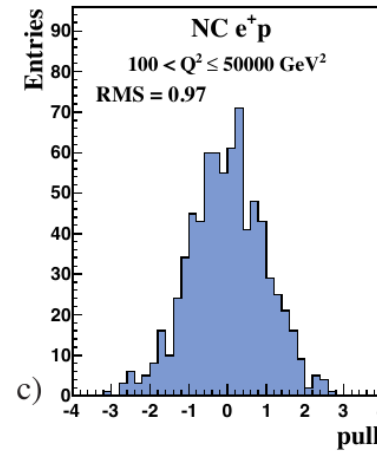
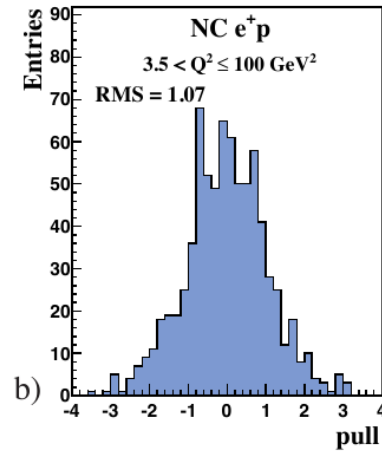
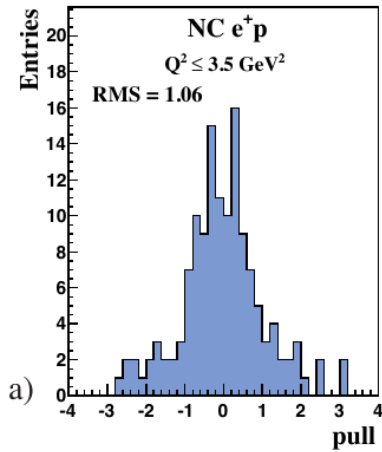
$$\sigma(x_{grid}, Q_{grid}^2) = \frac{\sigma_{model}(x_{grid}, Q_{grid}^2)}{\sigma_{model}(x_{meas}, Q_{meas}^2)} \cdot \sigma_{meas}(x_{meas}, Q_{meas}^2)$$

Data are also translated outside of region of DGLAP fit validity $Q^2 < 3.0$ GeV²

Use phenomenological "fractal" model and interpolate to DGLAP region

Other phenomenological fits tested \rightarrow negligible differences

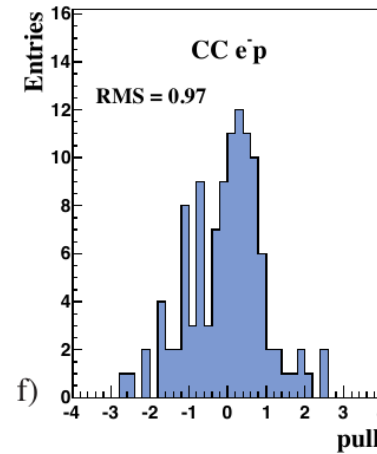
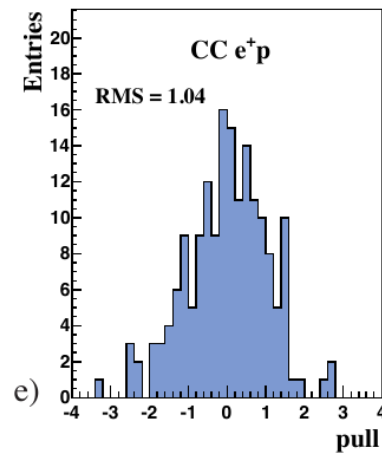
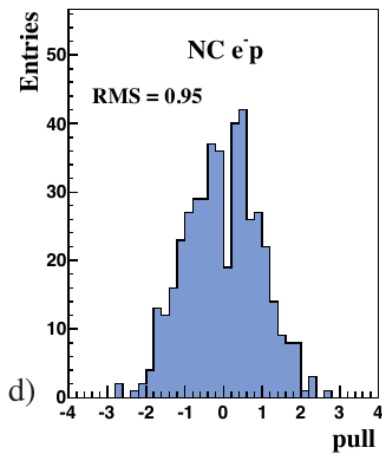
H1 & ZEUS data combination II



Overall $\chi^2/\text{ndf} = 1685 / 1620 = 1.04$

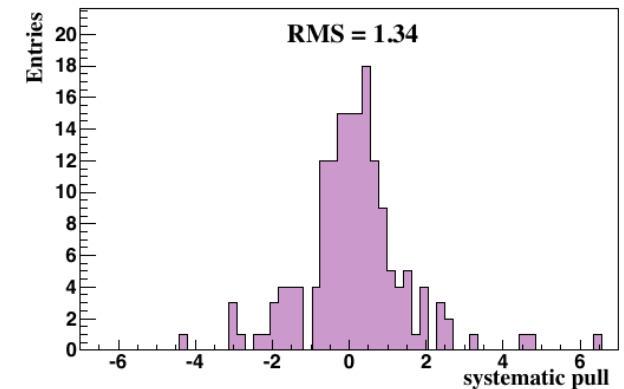
Pulls defined for each measurement difference between measured & average values after applying sys shifts b_j in units of uncorrelated uncertainty

Pulls of the data points should be distributed as a unit Gaussian



Each measurement channel shows pull centred on zero & unit width

pulls of the systematic sources b_j



$$p^{i,k} = \frac{\mu^{i,k} - \mu^{i,ave} (1 - \sum_j \gamma_j^{i,k} b_{j,ave})}{\sqrt{\Delta_{i,k}^2 - \Delta_{i,ave}^2}}$$

PDF extraction from data: HERAPDF2.0

HERAPDF1.0 & 1.5

Combine NC and CC HERA-I data from H1 & ZEUS
 Complete MSbar NLO fit
 NLO: standard parameterisation with 10 parameters
 NNLO HERAPDF 1.5 with 14p

HERAPDF2.0

Include additional NC and CC HERA-II combined data
 Complete MSbar NLO and NNLO fit
 NLO & NNLO fits require 15 parameters

$$xf(x, Q_0^2) = A \cdot x^B \cdot (1-x)^C \cdot (1 + Dx + Ex^2)$$

xg	xg	$xg(x) = A_g x^{B_g} (1-x)^{C_g},$	$xg(x) = A_g x^{B_g} (1-x)^{C_g} - A'_g x^{B'_g} (1-x)^{C'_g},$
xu_v	$xU = xu + xc$	$xu_v(x) = A_{u_v} x^{B_{u_v}} (1-x)^{C_{u_v}} (1 + E_{u_v} x^2),$	$xu_v(x) = A_{u_v} x^{B_{u_v}} (1-x)^{C_{u_v}} (1 + E_{u_v} x^2),$
xd_v	$xD = xd + xs$	$xd_v(x) = A_{d_v} x^{B_{d_v}} (1-x)^{C_{d_v}},$	$xd_v(x) = A_{d_v} x^{B_{d_v}} (1-x)^{C_{d_v}},$
$x\bar{U}$	$x\bar{U} = x\bar{u} + x\bar{c}$	$x\bar{U}(x) = A_{\bar{U}} x^{B_{\bar{U}}} (1-x)^{C_{\bar{U}}},$	$x\bar{U}(x) = A_{\bar{U}} x^{B_{\bar{U}}} (1-x)^{C_{\bar{U}}} (1 + D_{\bar{U}} x),$
$x\bar{D}$	$x\bar{D} = x\bar{d} + x\bar{s}$	$x\bar{D}(x) = A_{\bar{D}} x^{B_{\bar{D}}} (1-x)^{C_{\bar{D}}},$	$x\bar{D}(x) = A_{\bar{D}} x^{B_{\bar{D}}} (1-x)^{C_{\bar{D}}},$

HERAPDF1.0 & NLO HERAPDF1.5

HERAPDF2.0

$x\bar{s} = f_s x\bar{D}$ strange sea is a fixed fraction f_s of D at Q_0^2

Apply momentum/counting sum rules:

$$\int_0^1 dx \cdot (xu_v + xd_v + x\bar{U} + x\bar{D} + xg) = 1$$

$$\int_0^1 dx \cdot u_v = 2 \quad \int_0^1 dx \cdot d_v = 1$$

$$B_{\bar{U}} = B_{\bar{D}}$$

$$Sea = 2(\bar{U} + \bar{D})$$

$$A_{\bar{U}} = A_{\bar{D}}(1 - f_s)$$

ensures $x\bar{u} \rightarrow x\bar{d}$ as $x \rightarrow 0$

$$Q_0^2 = 1.9$$

$$Q_{\min}^2 = 3.5 \text{ or } 10 \text{ GeV}^2$$

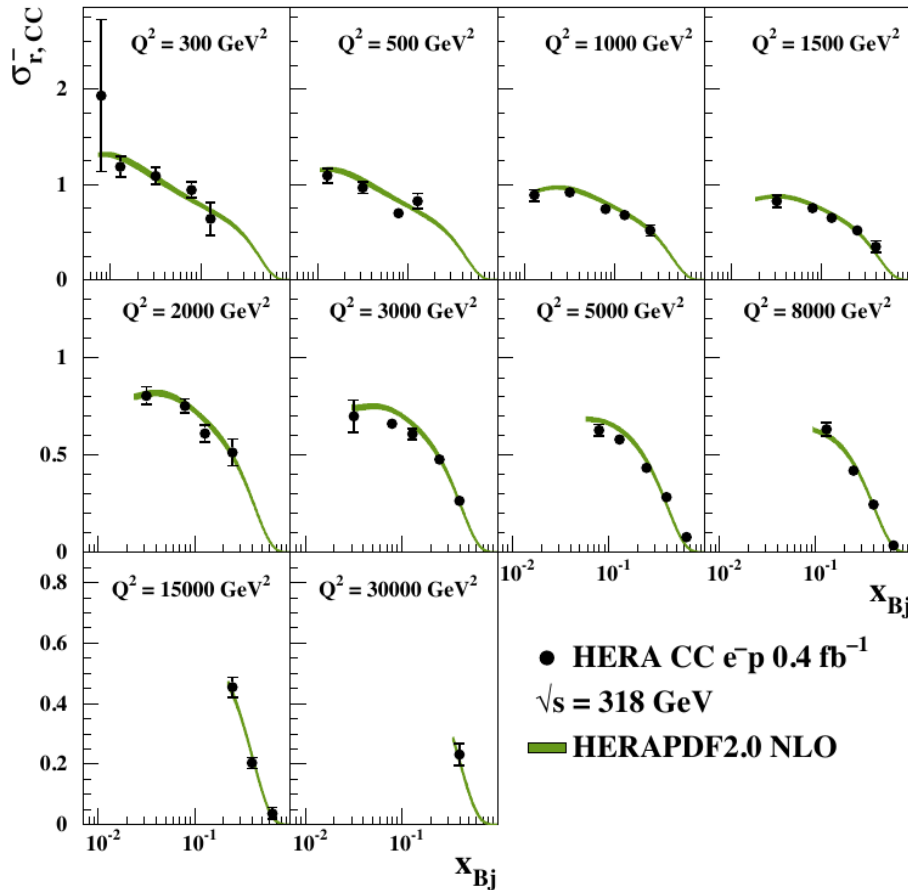
$$\alpha_s(M_z^2) = 0.118$$

$$2 \cdot 10^{-4} \leq x \leq 0.65$$

High Q^2 charged current cross sections

Electron scattering

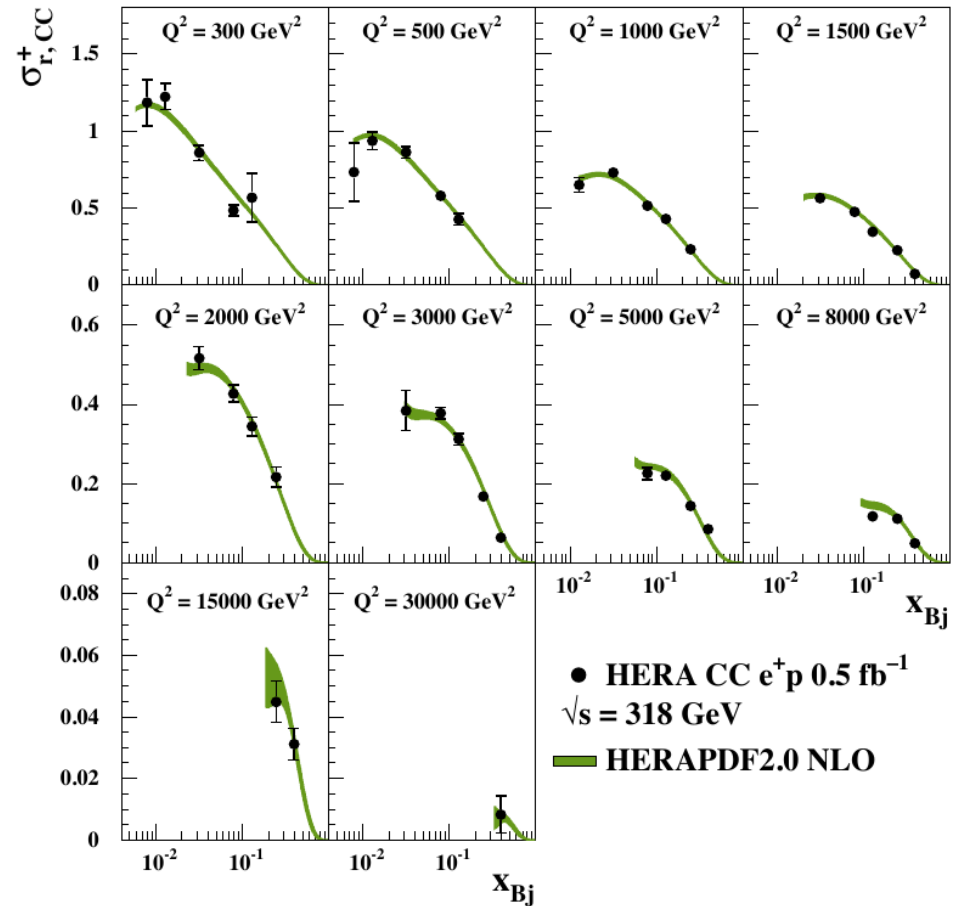
$$\frac{d^2\sigma_{CC}^-}{dx dQ^2} = \frac{G_F^2}{2\pi} \left(\frac{M_W^2}{M_W^2 + Q^2} \right)^2 \left[(u + c) + (1 - y)^2 (\bar{d} + \bar{s}) \right]$$



Combination of high Q^2 CC data (HERA-I+II)
 Improvement of total uncertainty
 Dominated by statistical errors
 Provide important flavour decomposition information

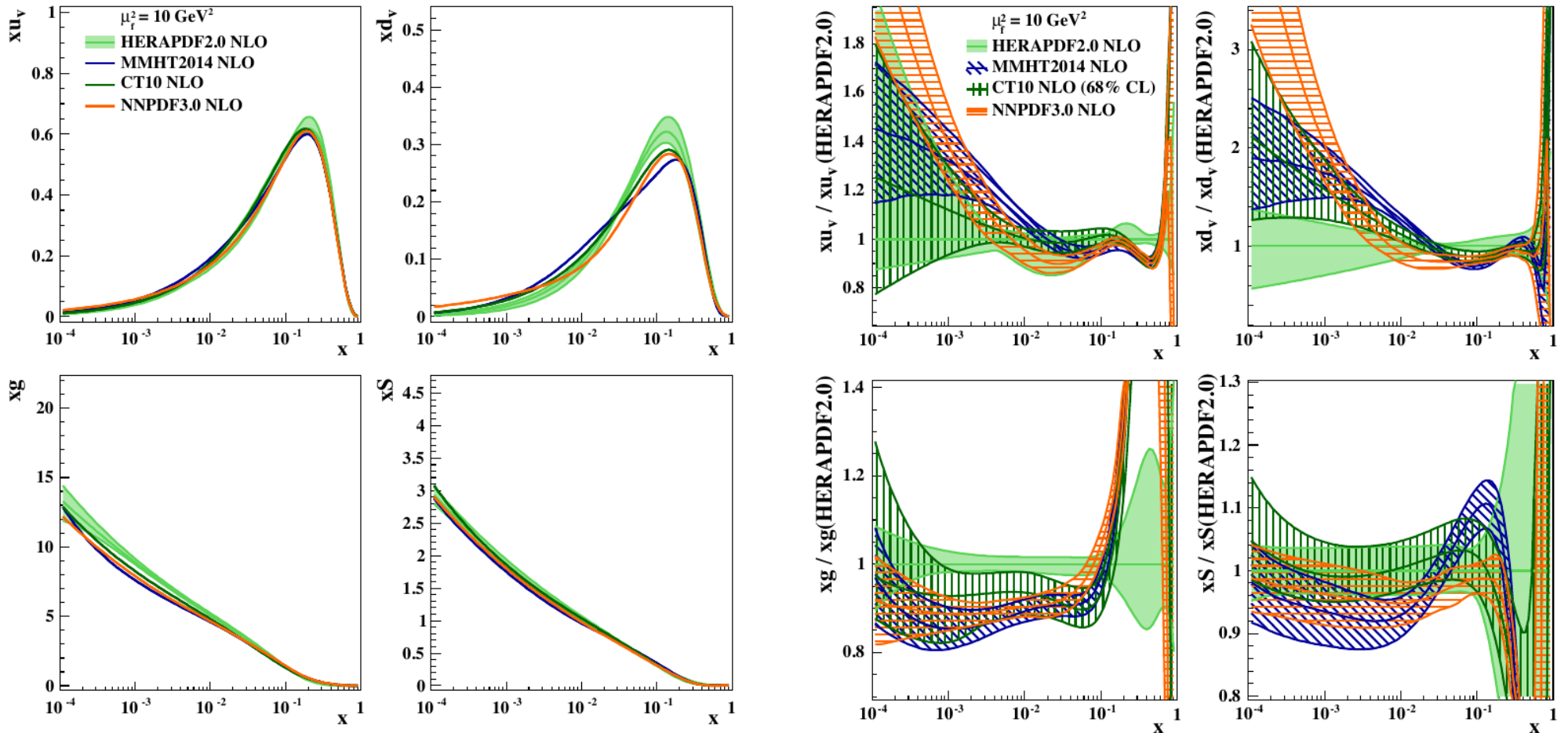
Positron scattering

$$\frac{d^2\sigma_{CC}^+}{dx dQ^2} = \frac{G_F^2}{2\pi} \left(\frac{M_W^2}{M_W^2 + Q^2} \right)^2 \left[(\bar{u} + \bar{c}) + (1 - y)^2 (d + s) \right]$$



CC e^+ data provide strong d_v constraint at high x
 Precision limited by statistics: typically 3-7%
 HERA-I precision of 10-15% for e^+

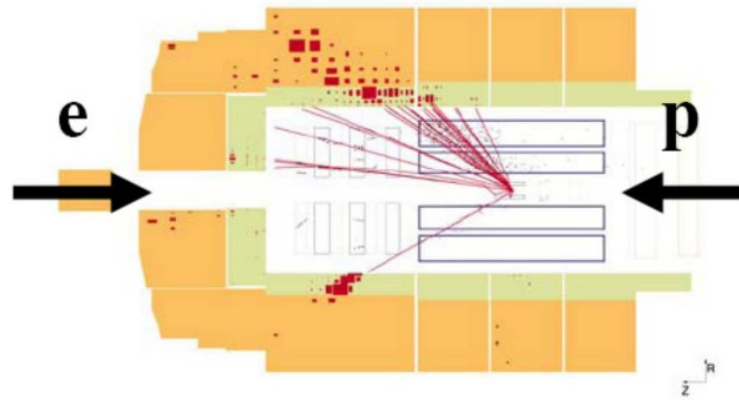
HERAPDF2.0 comparisons



Comparison of HERAPDF2.0 vs MMHT14 , NNPDF3.0 , CT10 (others use only HERA-1 combined data)
Differences at high x

- New HERA combined data improve precision at high x , Q^2
- HERAPDF uses proton target data only \rightarrow no nucleon / deuterium data
- Softer gluon at high x

NC and CC measurements



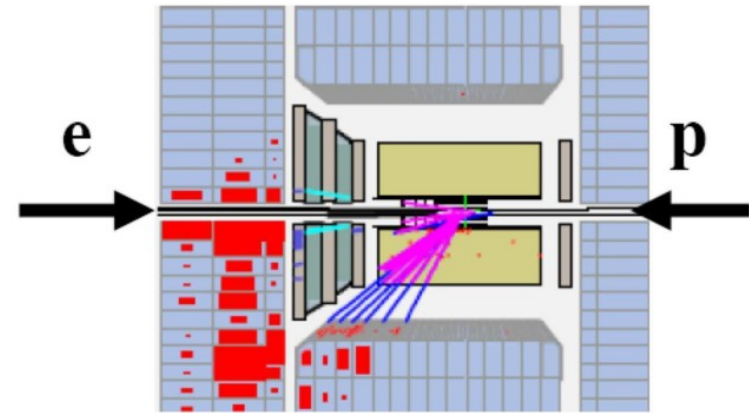
Neutral current event selection:

High P_T isolated scattered lepton
Suppress huge photo-production background by imposing longitudinal energy-momentum conservation

Kinematics may be reconstructed in many ways:
energy/angle of hadrons & scattered lepton
provides excellent tools for sys cross checks

Removal of scattered lepton provides a
high stats “pseudo-charged current sample”
Excellent tool to cross check CC analysis

Final selection: $\sim 10^5$ events per sample at high Q^2
 $\sim 10^7$ events for $10 < Q^2 < 100 \text{ GeV}^2$



Charged current event selection:

Large missing transverse momentum (neutrino)
Suppress huge photo-production background
Topological finders to remove cosmic muons
Kinematics reconstructed from hadrons
Final selection: $\sim 10^3$ events per sample

slide by E. Rizvi

Heavy flavor schemes

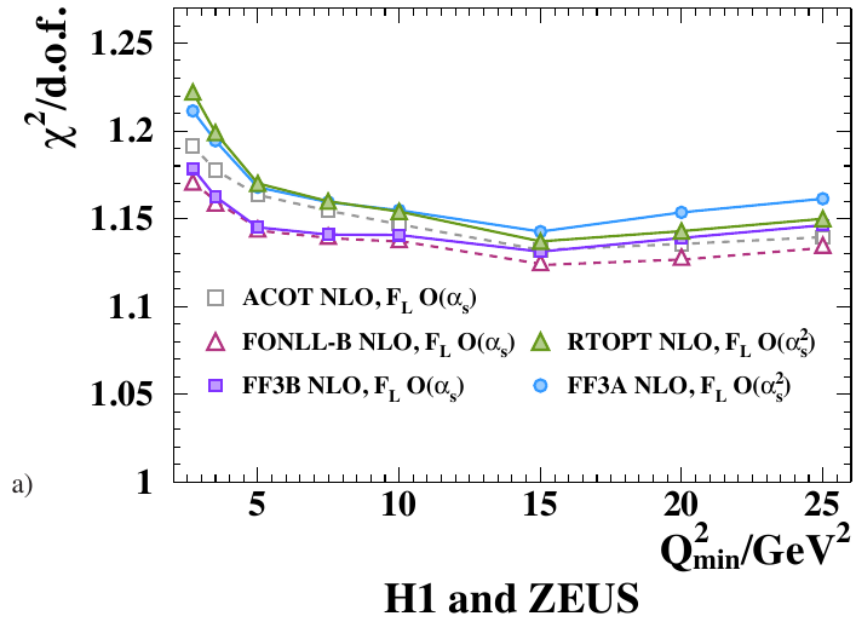
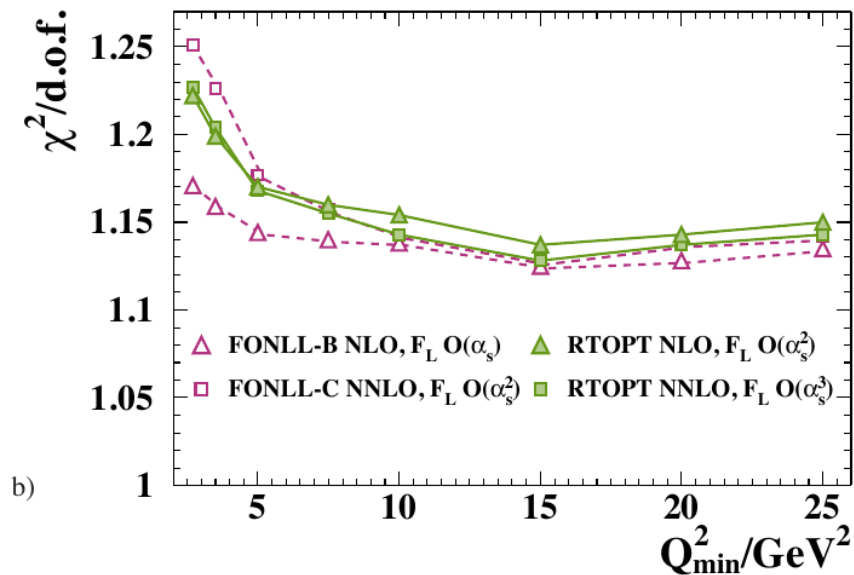
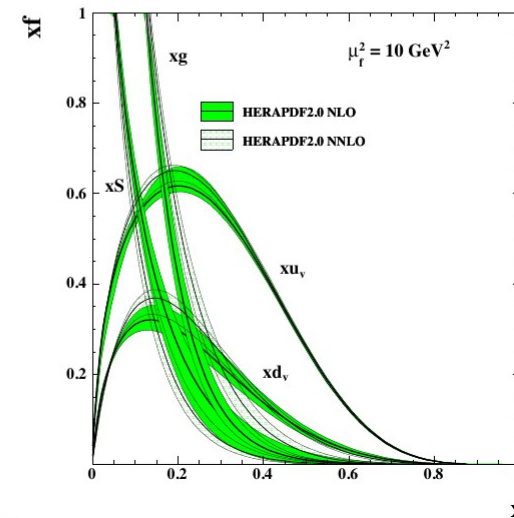
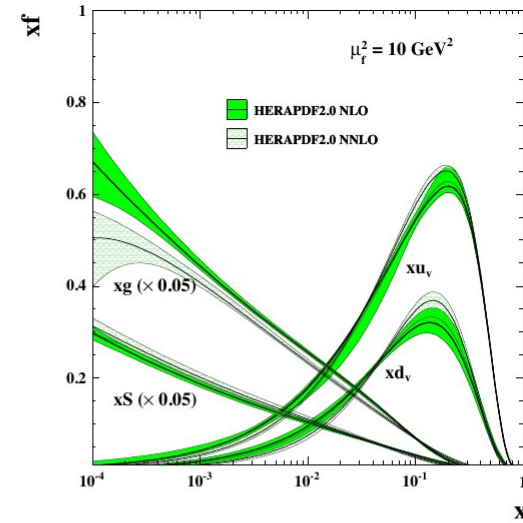
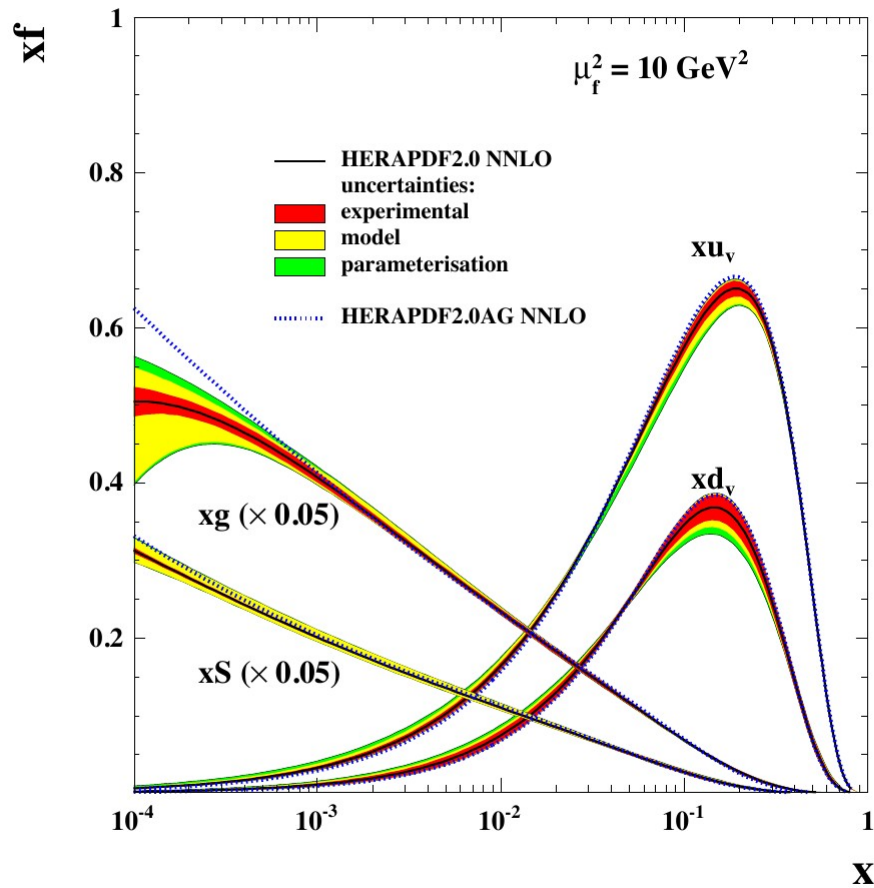


Figure 20: The dependence of $\chi^2/\text{d.o.f.}$ on Q_{\min}^2 for HERAPDF2.0 fits using a) the RTOPT [83], FONLL-B [90], ACOT [109] and fixed-flavour (FF) schemes at NLO and b) the RTOPT and FONLL-B/C [91] schemes at NLO and NNLO. The F_L contributions are calculated using matrix elements of the order of α_s indicated in the legend. The number of degrees of freedom drops from 1148 for $Q_{\min}^2 = 2.7 \text{ GeV}^2$ to 1131 for the nominal $Q_{\min}^2 = 3.5 \text{ GeV}^2$ and to 868 for $Q_{\min}^2 = 25 \text{ GeV}^2$.



HERAPDF2.0 NLO vs. NNLO



HERAPDF2.0 variants

The following variants of the HERAPDF2.0 PDFs have been released and will soon be available on LHAPDF (<https://lhapdf.hepforge.org>)

HERAPDF2.0 (NLO,NNLO, $Q^2_{\min}=3.5 \text{ GeV}^2$)

“Default PDF set”

- Data: combined HERA NC and CC inclusive cross sections
- HF Scheme: ROPT
- $\alpha_s(M_Z^2)=0.118$
- Grid with different $\alpha_s(M_Z^2)$ values (in the range [0.110-0.130] in steps of 0.01) are also released

HERAPDF2.0HiQ2 (NLO,NNLO)

“High- Q^2 version”

- as HERAPDF2.0 but with $Q^2_{\min}=10 \text{ GeV}^2$

HERAPDF2.0AG (LO,NLO,NNLO, $Q^2_{\min}=3.5 \text{ GeV}^2$)

“Alternative Gluon”

- Data: combined HERA NC and CC inclusive cross sections
- Use an alternative gluon parameterisation
- HF Scheme: ROPT
- $\alpha_s(M_Z^2)=0.130$ (LO) and $\alpha_s(M_Z^2)=0.118$ (NLO,NNLO)

HERAPDF2.0FF (NLO, $Q^2_{\min}=3.5 \text{ GeV}^2$)

“FF Schemes”

- Data: combined HERA NC and CC inclusive cross sections
- HF Schemes: Use two alternative (FF3A and FF3B) Fixed-Flavour schemes
- $\alpha_s(M_Z^2)^{N_f=3}=0.106573$ equivalent to $\alpha_s(M_Z^2)^{N_f=5}=0.118$ (FF3A) and $\alpha_s(M_Z^2)=0.118$ (FF3B)

HERAPDF2.0Jets (NLO, $Q^2_{\min}=3.5 \text{ GeV}^2$)

“Charm and Jets”

- Data: combined HERA NC and CC inclusive cross sections and selected HERA charm and jet production measurements
- HF Schemes: ROPT
- free $\alpha_s(M_Z^2)$ or $\alpha_s(M_Z^2)=0.118$